Aquaculture 598 (2025) 741951

Contents lists available at ScienceDirect

Aquaculture

journal homepage: www.elsevier.com/locate/aquaculture

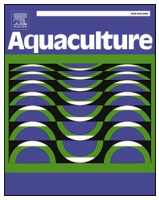

Deciphering the genetic basis and genomic prediction of heat tolerance trait from whole-genome resequencing in spotted sea bass (*Lateolabrax maculatus*)

Cong Liu [a,b], Haishen Wen [a,b], Chong Zhang [a,b], Yonghang Zhang [a,b], Lingyu Wang [a,b], Donglei Sun [a,b], Mengqun Liu [a,b], Yani Dong [a,b], Pengyu Li [a,b], Hao Li [a,b], Kaiqiang Zhang [a,b], Xin Qi [a,b], Yun Li [a,b,*]

[a] Key Laboratory of Mariculture, Ministry of Education (KLMME), Ocean University of China, Qingdao 266003, China
[b] Sanya Oceanographic Institution, Ocean University of China, Qingdao, Shandong/Sanya, Hainan 266100/572025, China

ARTICLE INFO

Keywords:
Lateolabrax maculatus
Heat tolerance trait
GWAS
Genomic selection

ABSTRACT

Spotted sea bass (*Lateolabrax maculatus*), widely farming in the China's coastal area, is a valuable fish species for aquaculture. Nevertheless, fluctuations in water temperature, particularly the significant increases during summer, threaten the survival and productivity of this species. Enhancing the heat tolerance of spotted sea bass is critical for ensuring the sustainable development of its aquaculture. In the present study, we undertook a genome-wide association study (GWAS) to explore the genetic basis underpinnings of heat tolerance in spotted sea bass. As shown in the results, 50 significantly associated genetic variants (31 SNPs and 19 InDels) were detected, distributed across multiple chromosomes, indicating that heat tolerance trait of spotted sea bass is governed by micro-effective multigene. Additionally, 236 candidate genes were also annotated, and *hspa5*, *mrpl13* and *ndufs8a* were identified as hub genes by PPI analysis. GO and pathway enrichment analyses indicated that membrane category and membrane trafficking pathway play a major role in the heat stress response. Furthermore, comparative evaluation of ten various genomic selection (GS) models and two selection strategies (GWAS-*p* and Random) revealed that the rrBLUP and SVM are optimal GS models for SNP and InDel markers, respectively. Overall, our findings deepen the knowledge of the molecular mechanisms of heat tolerance and highlights the potential of GS to boost heat tolerance performance in spotted sea bass and related species.

1. Introduction

Aquaculture is an emerging and vital industry that plays a crucial role in supplying animal protein and helping to bridge the existing gap between global demand and supply for essential proteins (Kobayashi et al., 2015). Since the early twenty-first century, global demand for 'blue foods' (aquatic foods) has nearly doubled (Naylor et al., 2021). However, the growing impacts of temperature fluctuations threaten aquaculture production significantly (Udayantha et al., 2023; Vermeer and Rahmstorf, 2009). Temperature is a fundamental and pivotal for fish among environmental factors, affecting various biological processes. Elevated environmental temperatures can lead to heat-induced shock, hypoxia, irreversible physiological injury, metabolic inhibition and internal energy imbalances in aquatic organisms (Chen et al., 2016; Rebl et al., 2013). Consequently, developing aquaculture traits related to thermal tolerance is critical to overcoming these challenges and ensuring the long-term sustainability of the aquaculture.

Recently, numerous studies have concentrated on uncovering the potential regulatory mechanisms involved in fish response to high-temperature stress, including immune (Zhou et al., 2021a, 2021b), antioxidant system (Forgati et al., 2017), behavioral (Corey et al., 2020), metabolic responses (Yang et al., 2020a, 2020b) and physiological (Jia et al., 2020). For instance, a study shown that adaptive and innate immune system activity were disrupted when exposed to simulated heatwaves in three-spined sticklebacks (*Gasterosteus aculeatus*) (Dittmar et al., 2014), while elevated temperature stress has been linked to histological structure damage and oxidative stress in pikeperch (*Sander lucioperca*) (Wang et al., 2019). In addition, *HSP70*, *UBI* and *CDKN1B* genes have been identified as regulator to thermal acclimation and response in goby fish (*Gillichthys mirabilis*) (Logan and Somero, 2011).

* Corresponding author at: Ocean University of China, No 5 Yushan road, Qingdao 266003, China.
E-mail address: yunli0116@ouc.edu.cn (Y. Li).

https://doi.org/10.1016/j.aquaculture.2024.741951
Received 26 September 2024; Received in revised form 6 November 2024; Accepted 25 November 2024
Available online 30 November 2024

These studies demonstrate that fish responses to thermal stress are multidimensional, with potential for adaptation to temperature fluctuations. However, there has been limited research on the genetic basis of thermal tolerance and its pragmatic applications for breeding heat-tolerant fish strains.

With the rapid advancements in genomic technology and genetic breeding research, the combination of genome-wide association study (GWAS) and genomic selection (GS) has emerged as a valid tool for the genetic enhancement of economical traits (D'Agaro et al., 2021; Fraslin et al., 2022). As an effective approach for associating biological phenotypes with genetics and elucidating the molecular mechanisms underlying target phenotypes, GWAS is widely applied to identify genes involved in multigenic traits for aquatic animals (Korte and Farlow, 2013), such as disease (Holborn et al., 2018), hypoxia (San et al., 2021), body shape (Kong et al., 2020), body color (Tang et al., 2023), growth traits (Yu et al., 2024) and sex determination (Gabián et al., 2019). Several GWAS investigations have uncovered a number of genetic variants linked to heat tolerance in fish. For instance, a GWAS study using the SNP array identified three SNPs significantly related to heat stress in catfish (*Ictalurus furcatus*), revealing 14 genes, including *TRAF2*, *PRPF4*, *DNAJC25*, *SLC25A46* and *PLCB1* (Jin et al., 2017). Nine SNPs significant related to heat tolerance were identified and four candidate genes predicted with the function of respiration, ion channels or obesity in northern pike (*Esox Lucius*) (Jiang et al., 2022). Additionally, GWAS studies on heat tolerance have been described in a variety of economic fish species, including large yellow croaker (*Larimichthys crocea*) and rainbow trout (*Oncorhynchus mykiss*) (Wu et al., 2021; Yoshida and Yáñez, 2022). GS, which is based on genome-wide association of variants to perform molecular marker-assisted selection (MAS) (Meuwissen et al., 2013), enables the assessment of breeding values through estimation of the effect of high-density markers (such as SNP or InDel) that cover the whole genome. Compared to traditional selective breeding techniques, GS possesses obvious advantages, including shorter breeding cycles and enhanced predictive performance, particularly for traits with low heritability and limited measurability (Xu et al., 2021). Successful applications of GS have been achieved in various fish breeding programs, including yellow drum (*Nibea albiflora*) (Liu et al., 2019), Atlantic salmon (*Salmo salar*) (Robledo et al., 2018), rock bream (*Oplegnathus fasciatus*) (Gong et al., 2022), Nile tilapia (*Oreochromis niloticus*) (Yoshida et al., 2019), large yellow croaker (Ke et al., 2022), hybrid red tilapia (*O. spp.*) (Sukhavachana et al., 2020) and European sea bass (*Dicentrarchus labrax*) (Vela-Avitúa et al., 2022), yielding substantial economic benefits. However, GS programs for these fish species have predominantly targeted growth or disease resistance traits, with limited investigation of high-temperature tolerance.

Spotted sea bass is extensively farmed along the Chinese coasts due to its enormous economic value (Zhang et al., 2023). However, this industry faces challenges from high summer temperatures. Exploring the genetic basis is essential to develop thermotolerant strains to improve the survivability for spotted sea bass under high temperatures. This study aimed to explore the genetic basis underpinnings of heat tolerance trait and assess the potential for GS in the future. To achieve this, we conducted a GWAS to identify the variants (SNPs and InDels) and candidate genes associated with heat tolerance based on a heating experiment. Subsequently, the predictive performance of distinct marker densities and GS models was evaluated for heat tolerance trait. Finally, the predictive performance of GS model using two different variants selection strategies was compared to determine the optimal GS breeding model for heat tolerance. Our findings enhance the comprehension of the genetic basis of thermal tolerance in spotted sea bass, and provide a solid groundwork for cultivating thermotolerant strains.

2. Materials and methods

2.1. Ethics statement

In this research, sample collection methods were designed according to the Guidelines for the Care and Use of Laboratory Animals in China, and agreed by the respective Animal Research and Ethics Committees of Ocean University of China (Permit Number: 20141201).

2.2. Heat treatment and sampling

In this study, cultured fish individuals of spotted sea bass sourced from Yantai Jinghai Marine Fisheries Co., Ltd. (Yantai, China), were used for heat stress experiments. The normal breeding conditions maintained at temperature of 22 ± 1 °C, salinity of 26.5 and dissolved oxygen level greater than 7.0 mg/ L. 500 healthy fish were randomly selected into five circular water circulation tanks for heat stress experiments. Fish were not fed during the entire thermal treatment period. A temperature control machine was run to precisely regulate the water temperature with an average heating rate of 1 °C / h until reaching 35 °C. Then, 35 ± 0.5 °C was set as stress temperature for 72 h due to the irreversible damage to fish caused by long-term high temperature. The reactions of the fish were meticulously monitored in the course of the heat treatment. The corresponding thermal tolerance time was recorded as phenotypic data whenever a fish loss of equilibrium (LOE) and failed to return to its normal posture within 10 s. The earlier the spotted sea bass exhibited LOE, the more sensitive to high temperature. After 72 h heat challenge, the phenotypic data of non-LOE fish individuals were recorded as 72 h. The pectoral fins of fish individuals were collected to extracted genomic DNA after anaesthetized by MS-222 (200 mg/L). Finally, 493 fish (body length: 25.96 ± 1.41 cm, body weight: 195.87 ± 32.98 g) were sampled during thermal challenge.

2.3. DNA isolation and sequencing

We isolated the genomic DNA from 493 individuals using commercially available kits. After measuring quantity and quality by a nucleic acid analyzer (OSTC, China), high-quality genomic DNA was stored at −20 °C for subsequent library construction. Library preparation was conducted using NEBNext® UltraTM DNA Library Prep Kit (NEB, USA). After library quality control, paired-end libraries with a 350 bp insertion length were prepared. Then, DNA library was sequenced on the DNBSEQ-T7 platform to produce paired-end 150 bp reads.

2.4. Genotyping and filtering

The raw sequencing data was quality assayed and filtered using fastp software (version 0.23.4) (Chen et al., 2018) to discard adapter contaminations and low-quality reads. After filtering, clean reads were generated and mapped to the genome sequence of spotted sea bass (PRJNA1045806) using BWA software (version 0.7.17) (Li, 2013). Variant calling was analyzed to obtain SNP and InDel (Insertion and deletion) variants using GATK (version 4.5.0.0) (McKenna et al., 2010). For hard filtering of SNPs, the parameters are as follows: QualByDepth (QD) < 2.0, FisherStrand (FS) > 60.0, RMSMappingQuality (MQ) < 40.0, ReadPosRankSumTest (ReadPosRankSum) < −8.0, MappingQualityRankSumTest (MQRankSum) < −12.5 and SOR ≥ 3.0, while for hard filtering of InDels, the parameters are as follows: QD < 2.0, MQRankSum < −12.5, FS > 200.0, ReadPosRankSum < −8.0 and SOR > 10.0. Thereafter, the PLINK software (version 1.9) (Purcell et al., 2007) was operated to further filter with parameters as follows: (1) missing rate per SNP (−-geno) < 0.01, (2) individual variant missing rate (−-mind) > 0.02, (3) minor allele frequency (−-maf) < 0.05, (4) Hardy-Weinberg equilibrium (−-hwe) < 0.001. For categorizing the effects of variant, the SnpEff software (version 5.0) was performed to annotate variants according to the annotated genomic locations of the genome of spotted

sea bass (Cingolani et al., 2012).

2.5. Linkage disequilibrium and population structure analyses

The PopLDdecay (version 3.42) was executed to calculated the linkage disequilibrium (LD) coefficient (r^2) between pairs of variants (SNP and InDel markers) for LD analysis (Zhang et al., 2019). Typically, the r^2 between variants on the genome declines as the marker distance increases. Strong correlation and high r^2 values are observed when two variants are located close to each other. The genome-wide LD decay pattern with distance was graphed using Plot_OnePop perl script from PopLDdecay software.

To assess the potential genetic relatedness within population, the population structure analysis was undertaken. Principal component analysis (PCA) of investigated sample was carried out by PLINK, and the PC1 and PC2 were plotted to exhibit the population structure. In addition, the Admixture (version 1.3.0) (Alexander et al., 2009) was further operated to calculate the population structure. The putative number of genetic group (K-value) was set to 1–15, and the optimal theoretical subgroup number was represented by the K-value with the smallest cross-validation error (CV) value.

2.6. Genome-wide association study

The GWAS analysis was performed with GEMMA (version 0.98.5) (Zhou and Stephens, 2012) based on the linear mixed model (LMM). Firstly, we obtained the genetic kinship between individuals with the parameter: -gk 2. Then, the generated genetic relatedness matrix was used for GWAS analysis, and the model was corrected with the results of the PCA analysis. The calculation formula is $y = W\alpha + X\beta + Z\mu + \varepsilon$ (Zhang et al., 2023). On the basis of Bonferroni correction method, the threshold was determined as 0.05/N for significant association and 1/N for suggestive association, where N is the total number of variants. Manhattan and quantile-quantile (Q-Q) plots were plotted using CMplot (version 4.5.10) (Yin et al., 2021) to visualize GWAS results. The phenotypic variance explained (PVE) value of the variants were calculated based on the published formula (Shim et al., 2015).

2.7. Candidate gene identification, enrichment and expression analysis

To identify genomic regions associated with significant variants linked to heat tolerance trait in spotted sea bass, we focused on regions positioned in 50 kb upstream and downstream of the relevant variants. The information of candidate genes was annotated using the BLAST software (version 2.15.0) against the NR, TrEMBL and Swiss-Prot datasets. For a deeper understanding of the response mechanisms of candidate genes, we performed Gene Ontology (GO) and pathway enrichment analyses using KOBAS tool (http://bioinfo.org/kobas) (Bu et al., 2021) with a statistical significance threshold of adjusted $P < 0.05$. Additionally, protein-protein interaction (PPI) network was constructed by uploading protein sequences of candidate genes to String (https://cn.string-db.org/) and identified hub genes using Cytoscape software (http://www.cytoscape.org/).

To investigate the expression of candidate genes after thermal excitation, liver (PRJNA1140113) and skeletal muscle (PRJNA1071322) transcriptome data under heat stress were analyzed. The transcriptome data were filtered to remove adaptor and low-quality reads using fastp, and then aligned with genome sequence using Hisat2 (version 2.2.1) (Kim et al., 2015). The FPKM value was calculated using StringTie (version 2.2.1) (Shumate et al., 2022). Based on the standard procedures of the DEseq2 software package (version 1.46.0) (Love et al., 2014), differential expression analyses were undertaken, $|\log2FoldChange| \geq 1$ and adjusted p-value ≤ 0.05 were set as the significant threshold.

2.8. Validation of the candidate genes

According to the heat tolerance time, fish sampled before heat stress (H0) and at 12 h (H12), 24 h (H24), 48 h (H48) and 72 h (H72) after temperature reached 35 °C were selected for further qPCR. Total RNA was isolated from the liver tissues using the Trizol method, and the RNA quality were evaluated using Biodropsis BD-1000 spectrophotometric absorbance (Beijing Oriental Science & Technology Development Ltd., China). Subsequently, RNA was reversed to cDNA as reaction template following the instructions (Takara, Japan). Specific primers of six candidate genes were listed in Supplementary Table 1, which were designed using Primer 5.0. Reference gene was *18S* gene, and all samples were tested in three replicates. The 10 μL qPCR reaction mixture was prepared with 1 μL of template cDNA, 5 μL of SYBR Premix solution (Vazyme, China), 0.5 μL of each prime, and 3.5 μL of nuclease-free water. qPCR was performed on the Applied Biosystems 7300 machines (Applied Biosystems, USA) under following conditions: initial denaturation at 95 °C for 3 min, followed by 40 cycles of 95 °C for 15 s, 60 °C for 30 s and 72 °C for 30 s. with a final extension at 72 °C for 5 min. The relative expression levels of tested genes were calculated with the $2^{-\Delta\Delta Ct}$ method. One-way analysis of variance (ANOVA) was performed, followed by Duncan's multiple range test, with statistical significance set at $P < 0.05$.

2.9. Heritability and correlation estimates

To calculate the heritability (h^2) of heat tolerance in spotted sea bass, the genomic relationship matrix was generated using GCTA (version 1.94.1) (Yang et al., 2011). The formula for evaluating narrow-sense heritability is $h^2 = \sigma_g^2 / \left(\sigma_g^2 + \sigma_e^2\right)$, where $\sigma_g^2$and σ_e^2 were the additive genetic variance and residual difference variance, respectively. Moreover, the phenotypic and genetic correlations of heat tolerance with growth traits (body length and body weight) were also assessed by ggstatsplot (R package, version 0.11.0) and GCTA software, respectively.

2.10. Genomic prediction

To evaluate the potential of GS, genomic prediction (GP) was conducted to assess the predictive accuracies of heat tolerance trait in spotted sea bass. For reducing the computational workload and given the strong correlations between neighboring SNPs or InDels in haplotype blocks, tagging variants were identified using PLINK software, which represent variants within haplotype blocks. Subsequent GP analysis was based on tagging variants. A total of ten models were applied for GP, including ridge regression BLUP (rrBLUP), five Bayesian models (Bayes A, Bayes B, Bayes C, BL: Bayes LASSO and BRR: Bayes ridge regression) and four machine learning models (GBM: Gradient-boosting machine, RF: random forest, SVM: support vector machine, and RKHS: reproducing kernel Hilbert space). The rrBLUP R package (version 4.6.3) (Endelman, 2011) was used to perform the rrBLUP prediction, the BGLR R package (version 1.1.1) (Pérez-Rodríguez, 2022) was used to calculate Bayesian and RKHS models, as well as the gbm R package (version 2.1.9) (Jerome, 2001), randomForest R package (version 4.7–1.1) (Breiman, 2001) and kernlab R package (version 0.9–32) (version 0.9–32) (Karatzoglou et al., 2004) were operated GBM, RF and SVM machine learning (ML) models, respectively.

By constructing 14 and 12 randomly sampled marker datasets with different numbers of SNP and InDel markers, respectively, the predictive accuracy of 10 GP models was compared using ten-fold cross-validation with five replicates. Briefly, 493 fish were randomly divided into non-overlapping sequential training populations ($n = 444$) and testing populations ($n = 49$) with a 9:1 ratio. The GP model was constructed using the training population and subsequently applied to estimate the genomic breeding values (GEBVs) for the testing population. Predictive

accuracy was defined as the average correlation coefficient between the observed phenotypic values and the predicted GEBVs generated from the prediction model. Subsequently, the predictive accuracy of randomly sampled datasets with five replicates for ten GP models was averaged across five replicates to minimize random effects.

For evaluating the effect of marker density on the predictive accuracy of distinct selection strategies, 12 and 10 marker subsets with different density were randomly sampled for SNP and InDel markers, respectively. The predictive accuracies were compared using two GS strategies as described below: (1) the informative variants selected by GWAS on the basis of *p*-values in ascending order which generated *via* GEMMA software (GWAS-*p*); (2) the informative variants selected randomly from the tagging SNPs or Indels (Random). In order to simulate the data more realistically, only the same number of fish as in the training population (n = 444) were selected for analysis with five replications. As mentioned earlier, the predictive accuracies were validated with ten-fold cross-validation.

3. Results

3.1. Phenotypic statistics of heat tolerance trait

LOE time of fish individual was considered as the thermal tolerance time from the stress temperature (35 °C). As illustrated by the survival curves in Supplementary Fig. 1, the first fish individual showing LOE was observed at 1.27 h. Subsequently, as the duration of exposure to high temperatures increased, fish individuals gradually exhibited LOE. Challenged Fish have high inter-individual variation in thermal tolerance traits, reflected the potential for artificial selection for heat tolerance in spotted sea bass.

3.2. Genotyping results, marker distribution and annotation

After genotyping and filtering, 3,769,461 SNPs and 644,400 InDels were detected among the all individuals using GATK software, and the histogram of minor allele frequency (MAF) distribution of SNPs and InDels were shown in Fig. 1A. Density map showed that SNPs and InDels were uniformly distributed across the 24 chromosomes (Fig. 1B). After annotation using SnpEff software, the genome-wide average change rate was calculated as 165 bp / SNP and 968 bp / InDel, respectively (Supplementary Table 2). Among those variants, 1,769,409 (38.77 %) SNPs and 321,698 (40.69 %) InDels were located in the intron region, 1,768,305 (38.75 %) SNPs and 304,989 (38.58 %) InDels were in the intergenic region, 162,496 (3.56 %) SNPs and 4327 (0.55 %) InDels were in the exon region, and 742,520 (16.27 %) SNPs and 137,843 (17.43 %) InDels were positioned in the gene coding region, respectively (Table 1).

Table 1
Variation annotation by genomic region, impact, and functional class.

Category	Type	SNP		InDel	
		Count	Percentage (%)	Count	Percentage (%)
Genomic region	Downstream	353,260	7.74	67,154	8.49
	Exon	162,496	3.56	4327	0.55
	Gene	0	0.00	7	0.00
	Intergenic	1,768,305	38.75	304,989	38.57
	Intron	1,769,409	38.77	321,698	40.69
	Splice site acceptor	202	0.00	108	0.01
	Splice site donor	252	0.01	113	0.01
	Splice site region	21,927	0.48	2980	0.38
	Transcript	0	0.00	71	0.01
	Upstream	389,260	8.53	70,689	8.94
	Utr_3_Prime	74,721	1.64	15,030	1.90
	Utr_5_Prime	23,759	0.52	3504	0.44
Impact	High	1076	0.02	2559	0.32
	Low	138,866	3.04	2980	0.38
	Moderate	48,286	1.06	1990	0.25
	Modifier	4,375,363	95.88	783,141	99.05
Function class	Missense	48,437	34.94	–	–
	Nonsense	480	0.35	–	–
	Silent	89,725	64.72	–	–

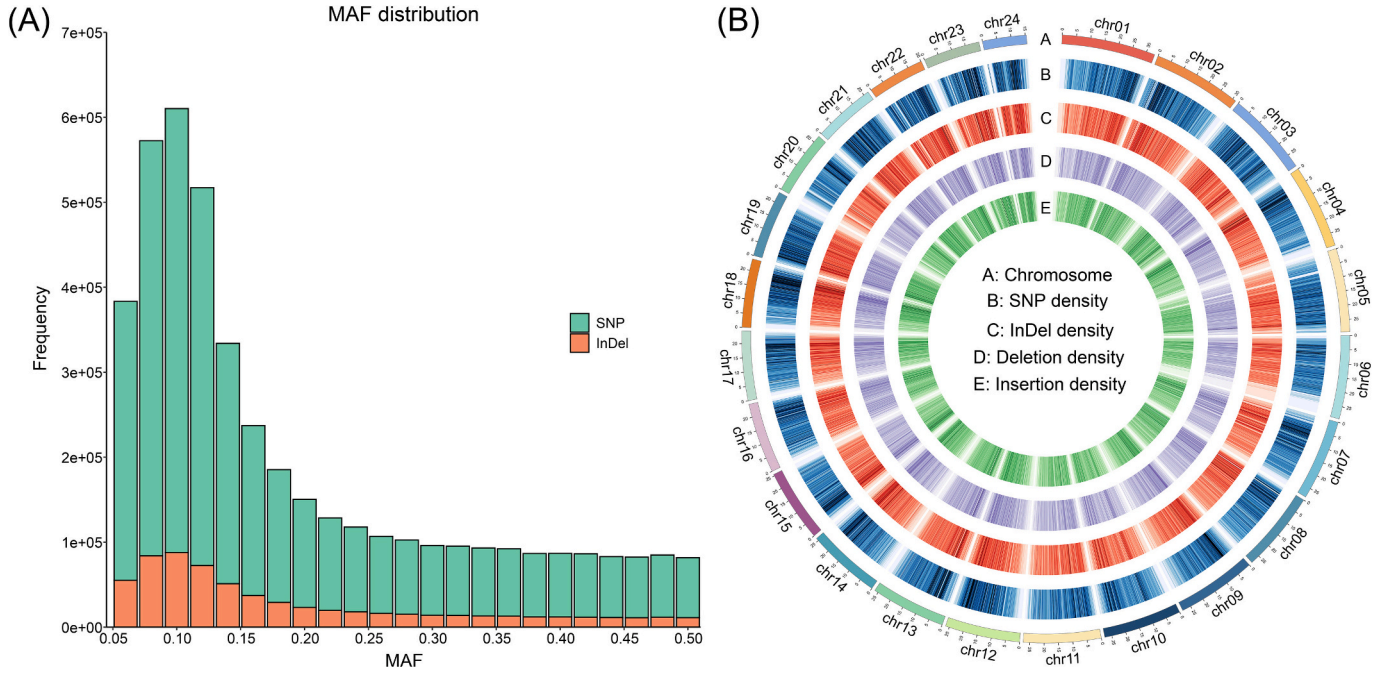

Fig. 1. The characteristics of detected variants in spotted sea bass. (A) The histogram of minor allele frequency (MAF) distribution. (B) Density and distribution of the high-quality SNPs and InDels among 24 chromosomes.

3.3. Population structure and LD analyses

As shown in Fig. 2A, the PCA analysis results suggested that there were several discrete subgroups, and can be roughly classified into two subpopulations. In the analysis of population structure, the CV continued to decrease as the value of K increased. The CV value reached its minimum when K = 12 (Fig. 2B), which was considered to be the theoretically optimal genetic subpopulation number, indicating a complex and diverse population structure. Weak genetic relatedness across experimental spotted sea bass was observed through the genetic relatedness matrix (Fig. 2C). Based on the LD analysis, the squared correlation coefficient (r^2) declined sharply with increasing distance between SNPs. The maximum r^2 value was 0.44, and quickly decreasing to 0.1 at a distance of 600 bp (Fig. 2D). Additionally, population structure analysis using InDel markers was conducted. The PCA results for InDel markers showed a similar pattern, revealing two distinct subgroups (Supplementary Fig. 2A), which supports the findings from the SNP analysis. The CV value for InDel markers also showed a decrease as K increased, reaching a minimum at K = 12, further confirming the presence of a complex population structure (Supplementary Fig. 2B). Similar to the SNP markers, the genetic relatedness matrix for InDel markers also indicated weak genetic relationships among the samples (Supplementary Fig. 2C). The maximum r^2 value was 0.86, and quickly decreasing to 0.1 at a distance of 700 bp (Supplementary Fig. 2D).

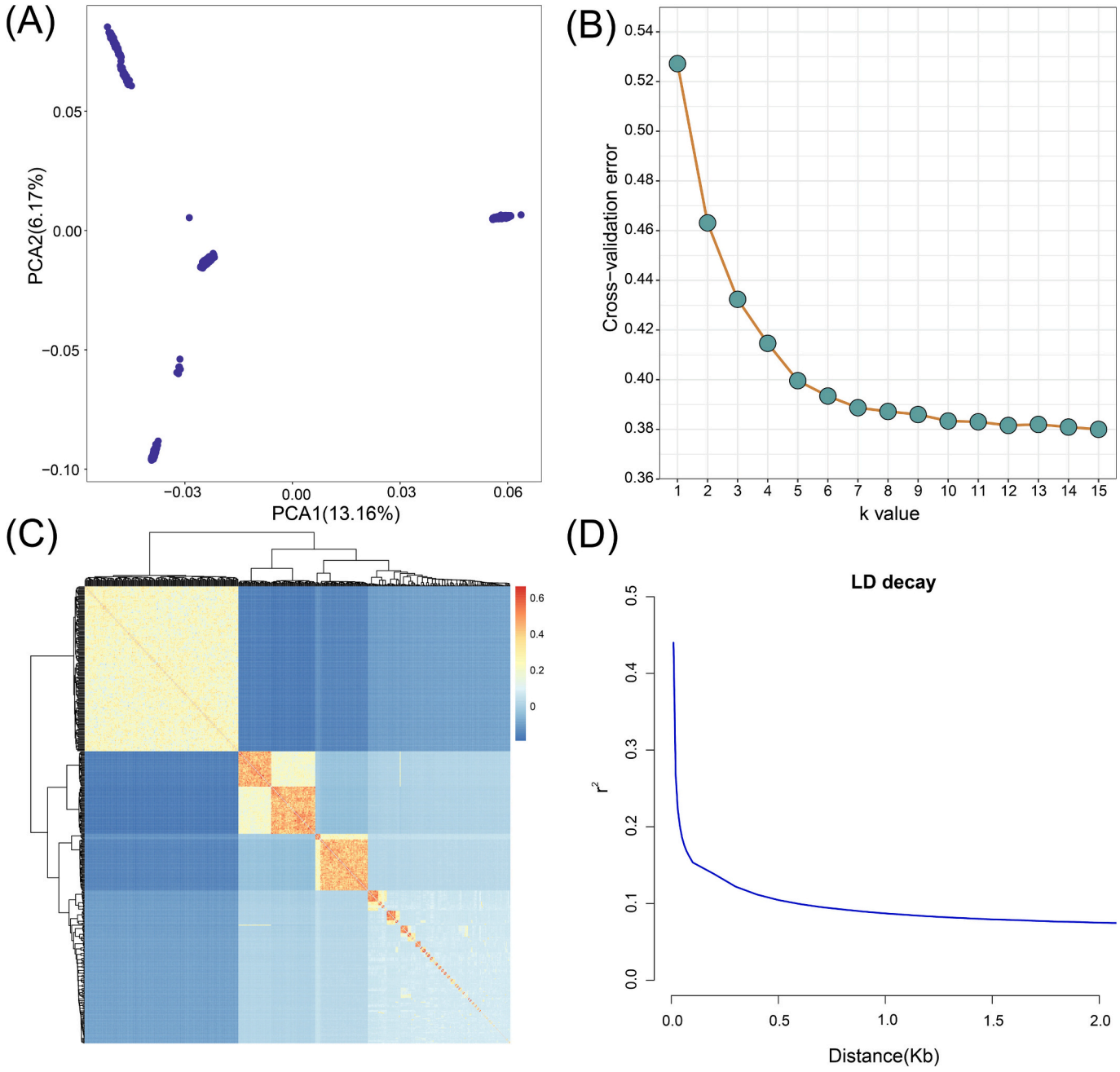

Fig. 2. (A) PCA plot of experimental fish based on the results of SNP marker analysis. Purple dots denote individuals used in GWAS analysis. (B) Variation of cross-validation error at different K values. (C) The heatmap of genetic relatedness among the challenged individuals. Blue indicated low relatedness and red indicated high relatedness (D) LD decay plot of SNPs. The Y-axis represents the squared correlation coefficient (r^2), the X-axis represents the physical location. (For interpretation of the references to color in this figure legend, the reader is referred to the web version of this article.)

3.4. Genome-wide association analysis

3,769,461SNPs and 644,400 InDels from 493 individuals were used for GWAS. The suggestive and significant statistical thresholds were set as $-\log_{10}(1/3769461) = 6.58$ and $-\log_{10}(0.05/3769461) = 7.88$ for SNP marker, while the suggestive and significant statistical thresholds were $-\log_{10}(1/644400) = 5.81$ and $-\log_{10}(0.05/644400) = 7.11$ for InDel marker, respectively. As a result, a total of 50 variants (31 SNPs and 19 InDels) were detected in association with heat tolerance trait of spotted sea bass, scattered on 17 chromosomes, including chr 2, 3, 4, 5, 6, 7, 8, 9,

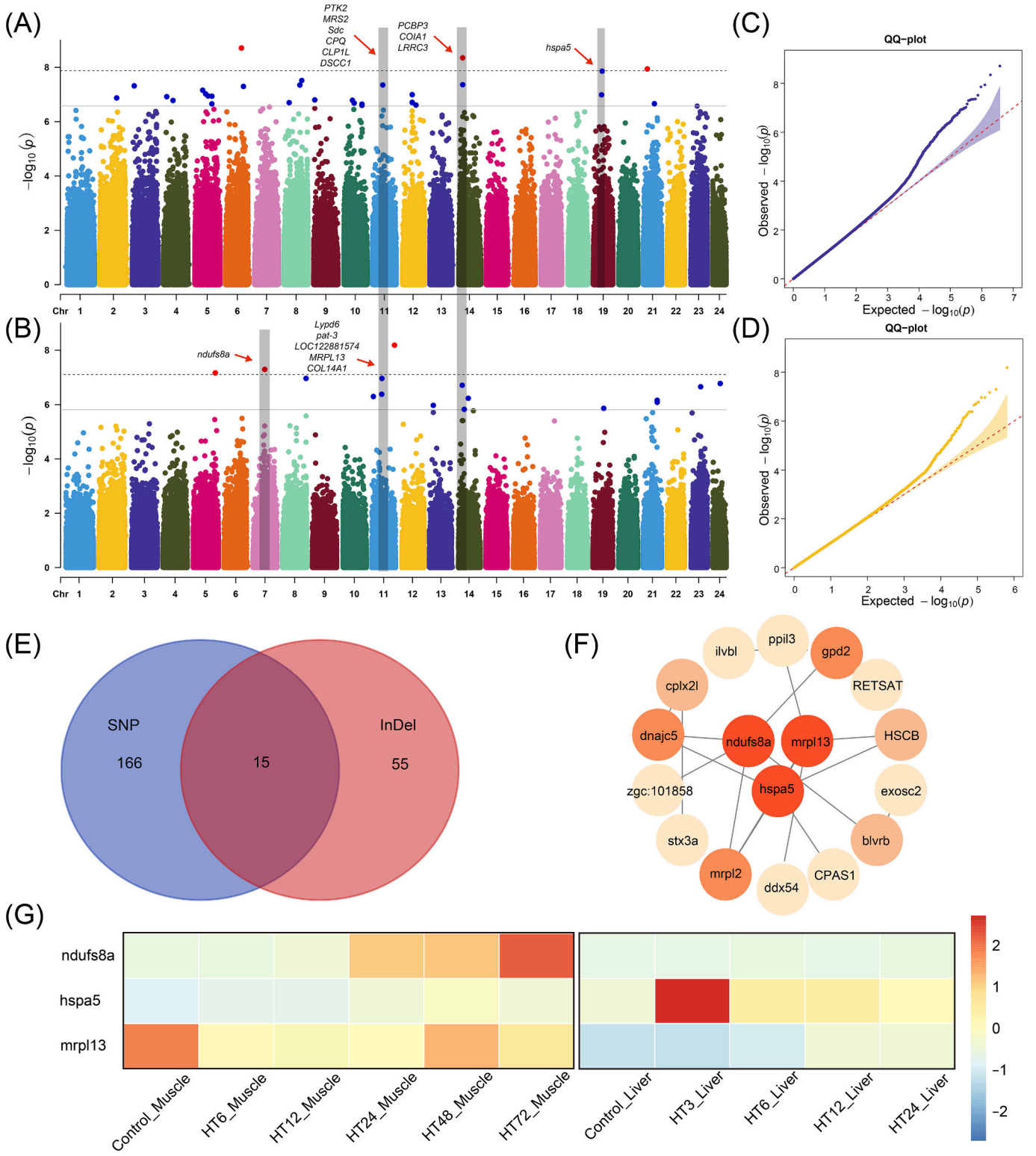

Fig. 3. GWAS analysis results for heat tolerance trait of spotted sea bass. Manhattan plot for SNP marker (A) and InDel marker (B), respectively. The dotted line of Manhattan plot represents the significance threshold. The solid line represents the suggestive threshold. Q-Q plots showed the validity of the GWAS analysis for SNP (C) and InDel marker (D), respectively. (E) Venn diagram of candidate genes associated with SNP and InDel variants. (F) Results of PPI analysis of candidate genes. (G) Heatmap of the expression of three hub genes in spotted sea bass liver and muscle tissues under thermal stress.

10, 11, 12, 13, 14, 19, 21, 23 and 24 (Fig. 3A and Fig. 3B). Among those variants, three SNPs and InDels were determined as significant correlations with heat tolerance trait, respectively, while the remaining variants were considered as suggestive correlations. The *p*-value of chr06:18472093 was the smallest among the 31 SNPs ($P = 1.94E-09$) with the PVE value of 7.59 % and minor allele frequency of 0.075. For InDels, the *p*-value of chr11:26014378 was the smallest ($P = 6.48E-09$) with the PVE value of 7.08 % and minor allele frequency of 0.084. Furthermore, most of the significant variants were positioned in the intron, upstream and intergenic region (account for 94.00 %), with only one significant SNP positioned in 3_prime_UTR, downstream and exon regions separately (Supplementary Table 3). As a confirmation of the reliability and validity of the GWAS analysis, Q-Q plots demonstrated that the statistical model was appropriate in this study (Fig. 3C and Fig. 3D).

After scanning the upstream and downstream 50 kb genomic regions, 236 candidate genes were annotated that are potentially related to heat tolerance trait in spotted sea bass (Supplementary Table 4). Among those genes, 15 candidate genes overlapped between SNP and InDel annotation results, 166 and 55 candidate genes were specific for SNP and InDel annotation, respectively (Fig. 3E). By constructing PPI network, we screened three highly connected candidates as hub genes, including *hspa5*, *mrpl13* and *ndufs8a* (Fig. 3F). The heatmap of three hub genes showed the dynamic changes of expression after heat stress (Fig. 3G).

3.5. Candidate gene validation and function enrichment analysis

To validate the results, the relative expression levels of six candidate genes were detected by qPCR, including *ABCA1* (ATP binding cassette subfamily aa member 1), *CPQ* (Carboxypeptidase Q), *ANKRD13D* (Ankyrin repeat domain 13 family, member D), *NUCB2* (Nucleobindin 2), *PAT-3* (Integrin) and *PNPLA2* (Patatin like phospholipase domain containing 2). The *ABCA1* and *PAT-3* genes were significantly up-regulated on H48. However, the *ANKRD13D* and *PNPLA2* genes were significantly down-regulated. The *CPQ* and *NUCB2* genes exhibited a tendency to be up-regulated (Fig. 4).

Furthermore, the GO and pathway enrichment analyses results indicated that the membrane term was significantly enriched, with a highest gene number (Supplementary Table 5). In addition, recycling endosome, synaptic vesicle, guanyl-nucleotide exchange factor activity and small GTPase mediated signal transduction were also significantly enriched. Interestingly, in the enriched pathways, membrane trafficking, vesicle-mediated transport, RAB GEFs exchange GTP for GDP on RABs, Golgi associated vesicle biogenesis, Rab regulation of trafficking, trans-Golgi network vesicle budding and Clathrin-mediated endocytosis pathways were also found (Supplementary Table 5 and Fig. 5), suggesting that membrane trafficking mechanisms are engaged in the molecular response to high ambient temperatures. Several genes involved in these pathways were drawn in Fig. 5, and their differential expression folds after thermal stress were shown in a heatmap, with asterisks denoting the significant differences. Based on enrichment analysis and literature search, a putative schematic diagram of the molecular mechanisms involved in the response of the spotted sea bass to high temperature stress through the membrane trafficking pathway is summarized, which illustrates the transport processes and of biochemical molecules (Fig. 6).

3.6. Heritability and correlations

Based on high-quality SNPs, heritability estimates of 0.13 ± 0.07 was obtained, indicating a low heritability for the heat tolerance trait of spotted sea bass (Table 2). Correlation analysis between the heat tolerance trait and two growth-related traits suggested very weak negative phenotypic correlations, with Pearson's correlation coefficients of -0.22 ($p = 7.94e-07$) for body length and -0.03 ($p = 0.49$) for body weight, respectively (Supplementary Fig. 3). Moreover, the genetic correlations of thermal tolerance time and body length and body weight were also respectively calculated using GCTA software, and the results showed weak negative genetic correlations were observed, with a correlation of -0.06 ± 0.31 for body length and -0.12 ± 0.30 for body weight, respectively (Supplementary Table 6).

3.7. Comparison of thermal tolerance time among different genotypes

For the purpose of investigating the superior genotype, the differences of SNPs and InDels significantly associated with heat tolerance trait of spotted sea bass were separately analyzed by combining

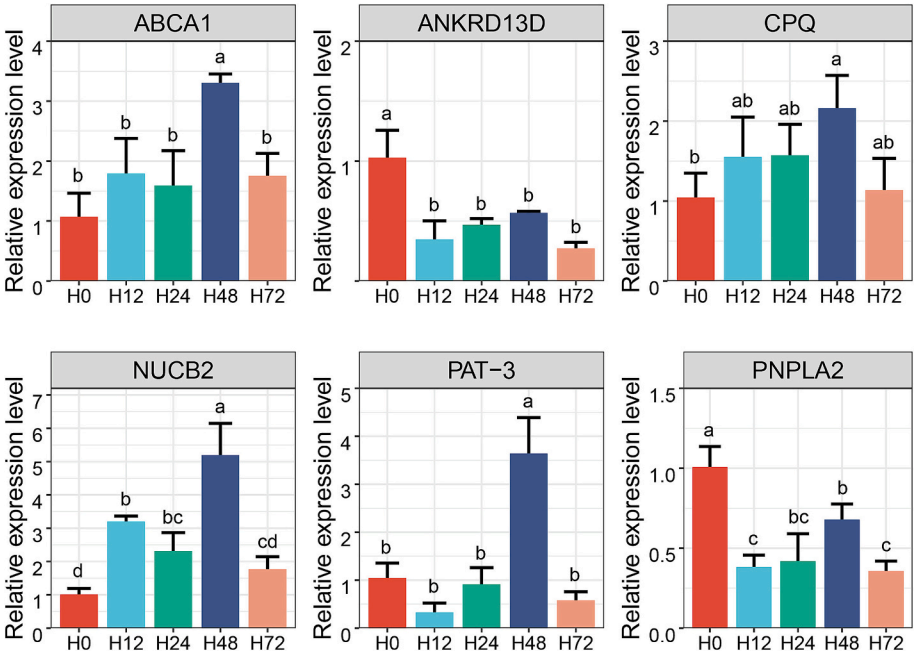

Fig. 4. Validation of six candidate genes by qPCR.

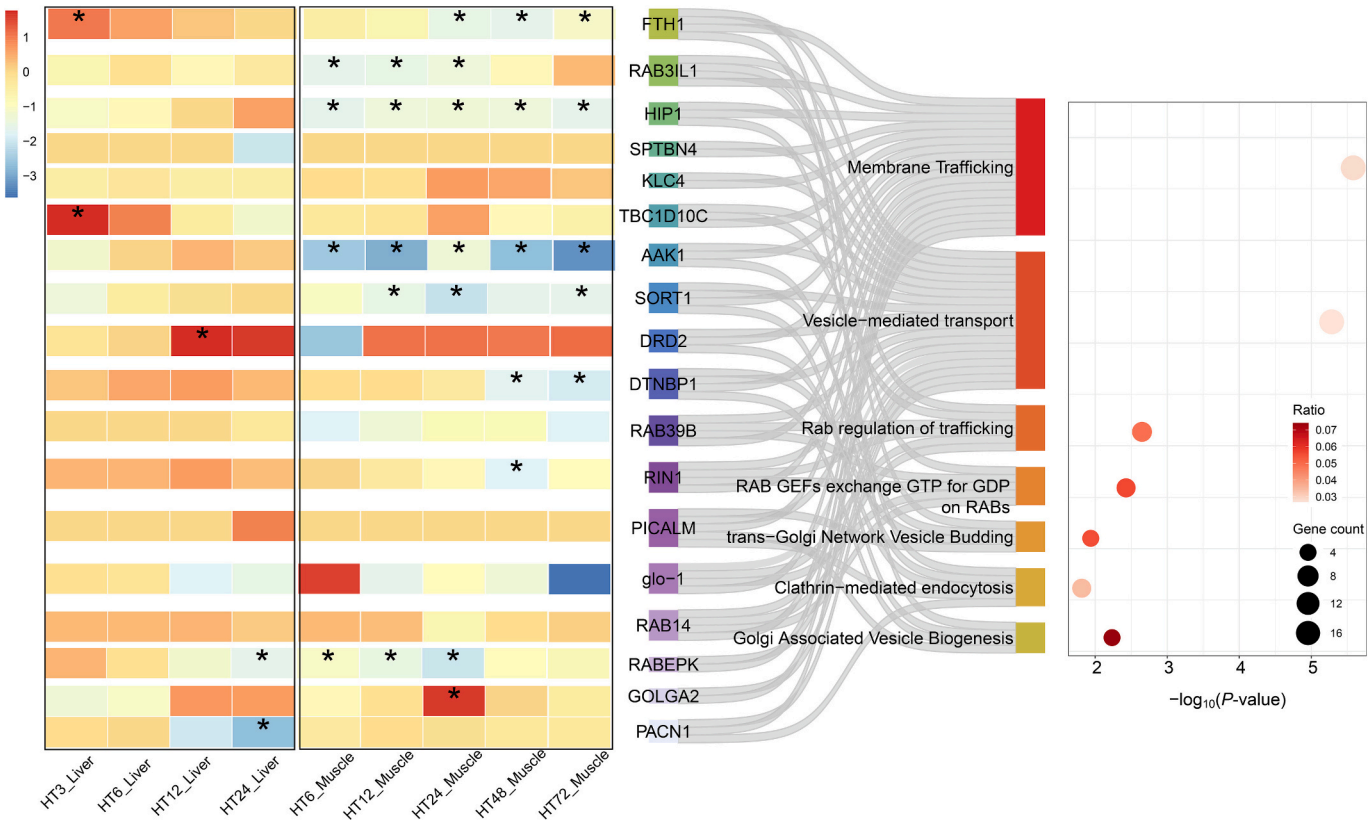

Fig. 5. Enrichment results related to membrane trafficking pathway. The heatmap exhibiting differential expression folds of genes enriched in the pathway in liver and muscle tissues after thermal shock.

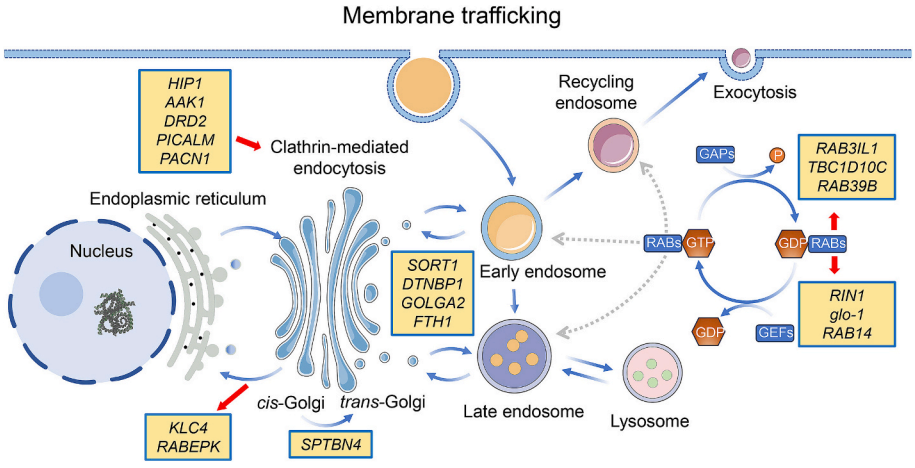

Fig. 6. Schematic diagram of the putative regulatory mechanism of the spotted sea bass in response to heat stress by membrane trafficking pathway.

Table 2
Results of the heritability analysis for heat tolerance trait using SNP markers.

Source	Variance	SE
V(G)	227,112.5071	132,140.7279
V(e)	1,475,235.675	134,438.3908
Vp	1,702,348.183	114,130.2727
V(G)/Vp	0.133411	0.07439

V(G): genetic variance among individuals; V(p): total phenotypic difference. V (e): environmental variance contributing to phenotypic differences.

individual thermal tolerance time and genotype data, respectively. Significant differences in the thermal tolerance time were observed among different genotypes (Fig. 7). For the three significantly associated SNPs (chr06:18472093, chr14:5187820 and chr21:4565319), individuals with the GG, AA, and CC genotypes exhibited significantly longer thermal tolerance times compared to those with other genotypes (Fig. 7A). For the three significantly associated InDels (chr05:25792997, chr07:13415682 and chr11:26014378), A/A and TTAA/TTAA were the superior genotype (Fig. 7B).

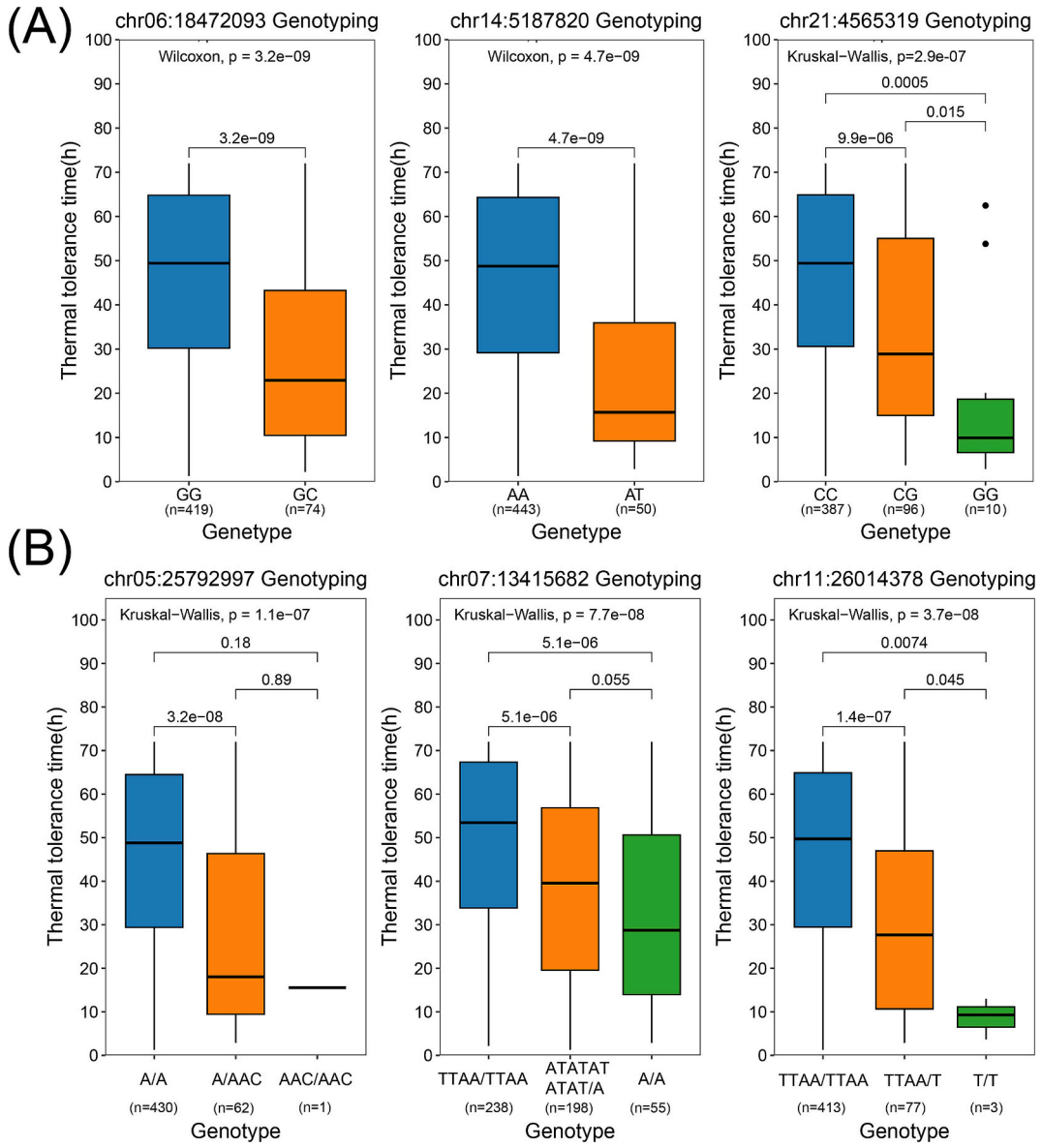

Fig. 7. Box plot of thermal tolerance time of 493 sequenced samples with different genotypes. (A) Results for three significantly associated SNPs. (B) Results for three significantly associated InDels. The Y-axis represents the thermal tolerance time of individuals, and different colors represent different genotypes. The n represents the number of individuals with different genotypes. Differences were analyzed using Wilcox and Kruskal tests.

3.8. Genomic prediction for heat tolerance trait

Based on the results of tagging analysis using PLINK software, 673,063 tagging SNPs and 104,419 tagging InDels were selected for genomic prediction, respectively. To evaluate the predictive accuracy of GEBVs, ten GS models were compared with ten-fold cross-validations through randomly selection of different numbers of tagging SNPs and InDels, respectively. It was revealed that the predictive accuracy of the testing populations was not increased with the increase of marker density (Supplementary Table 7 and Supplementary Table 8), rather it maintained at a low level. For both SNP and InDel, there are no strictly significant differences between the ten models, and one of the models may have better prediction accuracy at a specific marker density (Fig. 8). For instance, when the number of tagging SNPs was 6400, the highest predictive accuracy was observed in the rrBLUP model, while when the marker density is increased to 25,600, the BayesA model has the highest accuracy (Fig. 8A). Similar results were found in tagging InDel marker (Fig. 8B).

According to the results of the comparison of the two selection strategies (GWAS-*p* and Random), the general predictive performance of GWAS-*p* was superior to Random when using the same number of SNPs or InDels (Supplementary Table 9 and Supplementary Table 10). For the GWAS-*p* selection strategy, the predictive accuracy tended to increase and then decrease gradually with marker density from 10 to All. Conversely, for the selection strategy of Random, the predictive accuracy was consistently maintained at low values with increasing marker density, significantly lower than when using GWAS-*p* selection strategy. For SNP marker, the rrBLUP model reached a maximum predictive accuracy of 0.7734 ± 0.0260 at a marker density of 10 k, which was the highest among all models (Fig. 9A). While for InDel marker, the SVM model reached a maximum predictive accuracy of 0.7454 ± 0.0316 only at a marker density of 1 k (Fig. 9B). Both for SNP and InDel marker, the maximum predictive accuracy of the RF and GBM models was less than 0.6 (Supplementary Table 9 and Supplementary Table 10).

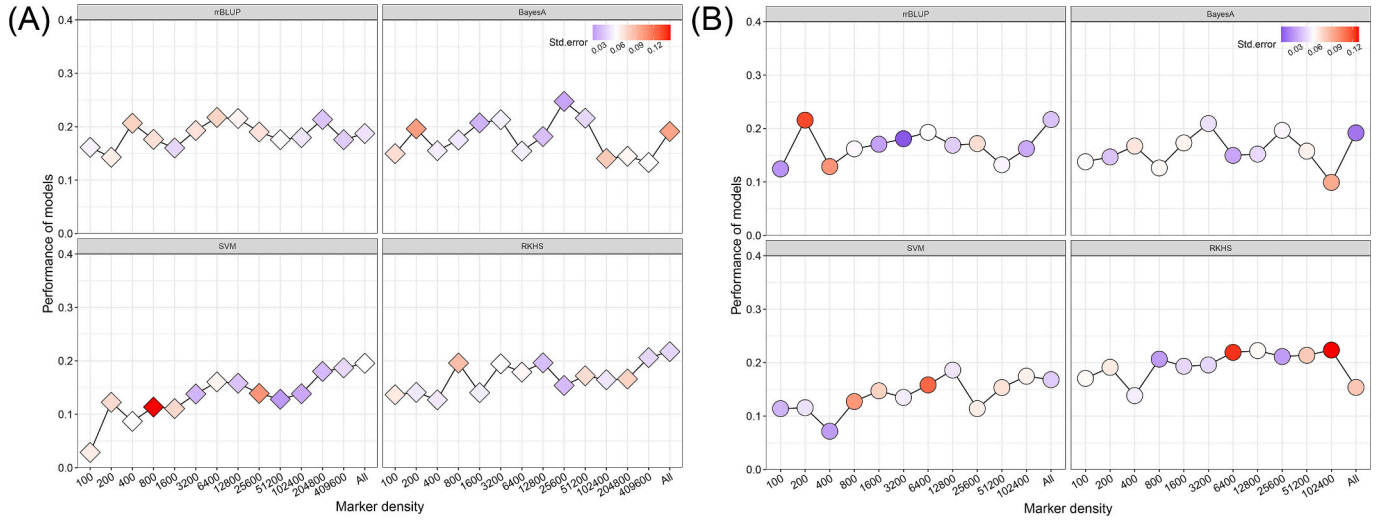

Fig. 8. Comparison of predictive accuracies of heat tolerance trait with different models using SNP (A) and InDel markers (B), respectively. Different colors and shapes represent standard errors and variant types, respectively.

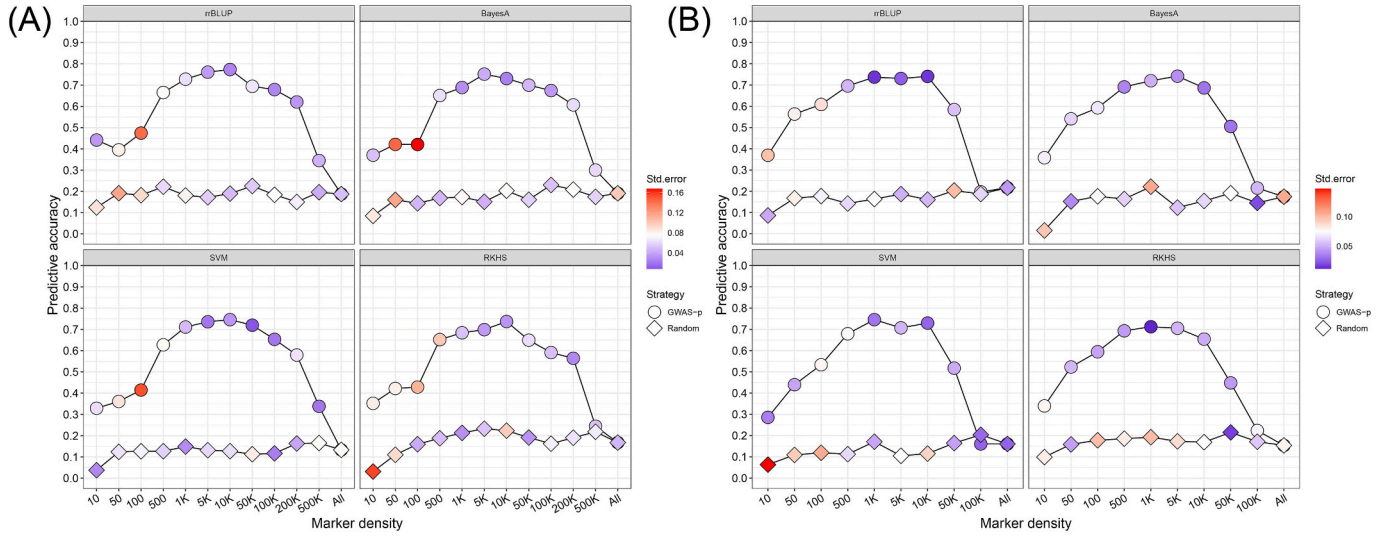

Fig. 9. Comparison of predictive accuracies using two selection strategies for heat tolerance trait using SNP (A) and InDel markers (B), respectively. Different shapes represent different selection strategies and different colors represent the size of the standard errors.

4. Discussion

Global warming generally causes higher water temperatures, posing significant challenges for fish. Acute fluctuations in water temperature can induce changes in fish physiological systems and their behaviors (Alfonso et al., 2021), exacerbate health problems and increase mortality, thereby dramatically impacting fisheries and aquaculture worldwide (Islam et al., 2022). Development of heat-tolerant trait aquaculture fish using a combination of GWAS and GS is a viable strategy to cope with the high-temperature challenge. GWAS has been applied for uncovering the genetic variations linked to economic traits and identifying candidates that regulate these traits, such as growth traits of brown-marbled grouper (*Epinephelus fuscoguttatus*) (Yang et al., 2020a, 2020b), head size of bighead carp (*Hypophthalmichthys nobilis*) (Zhou et al., 2021a, 2021b), disease resistance and black color traits of leopard coral grouper (*Plectropomus leopardus*) (Tang et al., 2023). In this research, we performed a GWAS to investigate the molecular mechanisms of heat tolerance and assessed the GP potential of development of molecular breeding markers in spotted sea bass.

From the GWAS results, 50 significant variants (31 SNPs and 19 InDels) were distributed across 17 chromosomes, indicating that heat tolerance trait in spotted sea bass are regulated by micro-efficient multiple genetic loci. During thermal stress, denatured proteins can form aggregates that are toxic to cells. Therefore, the degradation and elimination of misfolded proteins and damaged biomolecules are essential for fish to effectively respond to thermal stress (Kumar et al., 2022). There is widespread transcriptional evidence that heat shock proteins (HSPs) respond to heat stress by removing denatured proteins and safeguard cellular integrity (Jeyachandran et al., 2023). In a GWAS analysis in large yellow croaker, three HSP genes (*hsf1*, *dnajb4* and *hikeshi*) were considered as candidates for association with heat tolerance trait (Wu et al., 2021). From the GWAS results in our study, *hspa5* and *DNAJC5*, both members of the HSP family, were identified among 236 candidate genes. The *hspa5* gene encodes a heat shock protein 70 (HSP70) protein, plays a key role in the folding and assembling of proteins in the lumen of the endoplasmic reticulum (ER) and serves as a primary regulator of ER homeostasis. Published studies have shown that the relative expressions of *hspa5* significantly increases after heat stress in the spotted sea bass muscle, gill and liver tissues (Sun et al., 2021). Furthermore, the crucial role of the *hspa5* in responding to elevated

temperatures has been described in other fish, including Chinese tongue sole (*Cynoglossus semilaevis*) (Wang et al., 2024), olive flounder (*Paralichthys olivaceus*) (Kim et al., 2021) and spotted seatrout (*Cynoscion nebulosus*) (Song and McDowell, 2021). *DNAJC5* is one of HSP40 family members and functions in many cellular processes, such as membrane trafficking and protein folding by regulating the ATPase activity of the HSP70 (Paul et al., 2022). For instance, the methylation level of *DNAJC5* was observed to be different between control and heat-stressed groups in pig, identifying its involvement in processes related to cellular defense and stress response (Hao et al., 2016). Overall, the heat shock protein family genes exert a key role in the response to heat stress.

As hub candidate genes, *mrpl13* (mitochondrial ribosomal protein L13) and *ndufs8a* (NADH: ubiquinone oxidoreductase core subunit S8) were highlighted for their association with mitochondria function. *Mrpl13*, encoded by nuclear genes, is involved in protein synthesis, mitochondrial translation and metabolism of proteins within the mitochondrion. In clinical therapy, *mrpl13* has been shown to promote the proliferation of cancer cells and serves as potential prognostic marker (Jing et al., 2021). In aquaculture species, cardiac mitochondrial function in New Zealand wrasse (*Notolabrus celidotus*) was significantly altered by adaptation to summer temperatures (Iftikar et al., 2015). The *ndufs8a* gene encodes a subunit of mitochondrial NADH: ubiquinone oxidoreductase and is an essential component of the mitochondrial membrane respiratory chain NADH dehydrogenase (Haack et al., 2012). This complex uses ubiquinone as an electron acceptor to catalyze electron transfer from NADH through the respiratory chain. Liver transcriptomic analysis after heat stress treatment revealed the relative expression levels of the *ndufs8a* gene was significant decrease in large yellow croaker (Qian and Xue, 2016). Similarly, the transcript of *ndufs8a* was induced by heatwaves in a clam species (*Ruditapes philippinarum*) (García-Souto et al., 2024). It is well established that mitochondria are vulnerable to heat stress (Marquez-Acevedo et al., 2023). Mitochondria provide energy to the cell through oxidative phosphorylation, and mitochondrial energy production is typically disrupted under high temperatures. We speculate that the *mrpl13* and *ndufs8a* genes respond to heat stress by regulating the synthesis of ATP.

Cellular and organelle membranes are composed of a phospholipid bilayer that contains cholesterol and other lipids, where numerous biochemical reactions and processes occur (Hazel, 1995). GO enrichment of candidate genes showed significant enrichment of membrane category with the highest number of enriched genes, suggesting that membrane function may be influenced under heat stress. For instance, in black rockfish (*Sebastes schlegelii*), numerous differentially expressed genes (DEGs) exhibiting potential effects in adaptation to heat stress were categorized into membrane category (Lyu et al., 2018). Similarly, membrane term was also significantly enriched in grass carp under high temperature conditions (Zhang et al., 2022). Interestingly, the membrane trafficking pathway was significantly enriched in the pathway enrichment analysis of the candidate genes (Fig. 5). Membrane trafficking is the process by which macromolecules are delivered to the cell surface through membrane-bound vesicles (Lippincott-Schwartz et al., 2000). This pathway comprises several organelles, including the ER, plasma membrane, tubulovesicular transport intermediates and Golgi complex. Membrane trafficking between these organelles following highly organized routes, including clathrin-mediated endocytosis, ER to golgi anterograde transport, trans-golgi network vesicle budding, Rab regulation of trafficking, intra-golgi and retrograde golgi-to-ER traffic and endosomal sorting complex required for transport. For instance, proteins are synthesized and assembled in the ER and then delivered into the Golgi complex for maturation. After that, this protein is sorted in the trans Golgi network and then packaged into endosomes that fuse with the cell surface through the cytoplasm. For the exogenous macromolecules, clathrin-mediated endocytosis plays a significant role in controlling the uptake of materials from the plasma membrane, which are then delivered into the endosome. Useless or conformationally incorrect substances are digested by lysosomes. The key regulators of intracellular membrane trafficking are the Rab proteins, which contributes to the specificity of trafficking by localizing to the membranes of distinct organelles and interacting with effectors (Stenmark, 2009). The specific organelle response to heat stress has been demonstrated in earlier researches. For example, ER stress was induced by heat in the largemouth bass liver (*Micropterus salmoides*) (Zhao et al., 2022), and golgi apparatus were found to be involved in the response to the marine heatwave in the liver of *Acanthochromis polyacanthus* (Chan et al., 2022). Evidence has also been reported in the goby fish, where several Rab genes were induced or repressed expression by heat stress, mediating retrograde golgi-ER transport (Buckley et al., 2006). Overall, membrane trafficking responds to thermal excitation by delivering a range of macromolecules.

Heritability is central for genomic selection programs to pass traits sustainably to offspring (Bennett et al., 2014). The estimated heritability of heat tolerance trait has varied among species. For example, a high heritability value ($h^2 = 0.47$) was estimated for high-temperature tolerance, with LOE as the endpoint in Atlantic salmon (Benfey et al., 2022). Similarly, the heritability of resistance to acute high temperature were 0.325 in Pacific abalone (*Haliotis discus hannai*) and 0.29 in rainbow trout (Lagarde et al., 2023; Yu et al., 2021). Conversely, a low heritability of survival after heat shock challenge was observed with a value of 0.15 in Pacific oyster (*Crassostrea gigas*) (Camara et al., 2017). Heritability estimates are influenced by various factors, including species, populations, degree of inbreeding, genetic background, maternal effect, statistical models and trait measurements (Ødegård et al., 2011; Omeka et al., 2022). Notably, four different populations of turbot (*Scophthalmus maximus*) exhibited distinct heritability values (0.239 ± 0.141, 0.111 ± 0.080, 0.075 ± 0.026, and -0.019 ± 0.011) for heat tolerance trait (Ma et al., 2018). Additionally, in Zhikong scallop (*Chlamys farreri*), the heritability of heat tolerance traits differed between survival status (0.52 ± 0.04) and survival time (0.24 ± 0.03) (Yu et al., 2023). The heritability of heat tolerance in spotted sea bass in our study was estimated to be 0.13 ± 0.07, which is similar to the heritability of rainbow trout (0.13 ± 0.04) for survival under chronic thermal stress (Gallardo-Hidalgo et al., 2021), suggesting that it was strong influenced by environmental factors. Given the absence of prior studies on heat resistance in spotted sea bass, comparisons of heritability values across populations and trait measurements were not feasible. Nevertheless, despite the low heritability for heat tolerance trait in spotted sea bass, genome-wide selection breeding strategy could still be applied to boost heat tolerance performance.

GS has been demonstrated to be efficacious method for improving economic traits in fish, including female reproduction traits in rainbow trout (D'Ambrosio et al., 2020), disease resistance in Japanese flounder (Liu et al., 2018) and heat tolerance in Zhikong scallop (Yu et al., 2023). In this study, the predictive accuracy was assessed for thermal tolerance in spotted sea bass using rrBLUP, Bayes A, Bayes B, Bayes C, BL, BRR, SVM, RKHS, GBM and RF models. It was shown that the predictive accuracy of both SNP and InDel markers maintained low values at different marker densities. In contrast, GP for growth traits in spotted sea bass indicted that the predictive performance of the rrBLUP model outperformed the Bayesian models at different SNP densities (Zhang et al., 2023). For heat tolerance in abalone (Liu et al., 2022; VanRaden, 2008), the accuracy of Bayes B model prediction was superior to that of GBLUP model (produces the same result as rrBLUP). In Zhikong scallop, the prediction accuracies of the four models for survival status under thermal stress were ranked as follows: GBLUP > Bayes B > Bayes C > Bayes A (Yu et al., 2023). In addition to BLUP and Bayesian models, machine learning algorithms (ML) have also been used for genomic prediction, including SVM, RKHS, GBM and RF models. However, these ML models failed to show a superior prediction performance than BLUP and Bayesian models. The effectiveness of ML model is contingent upon high quality and sufficiently large training data. Although the predictive accuracy of ML models was affected by both training population size and marker density, increasing training population size improves genomic predictive performance more effectively than increasing marker density,

which was demonstrated in four growth traits in Bay scallops (*Argopecten irradians*) using ML models prediction (Zhu et al., 2021). In this study, larger training population sizes may be desirable for ML models to improve predictive accuracy. Generally, the accuracy of GP is influenced by various factors, including the number of genes affecting traits, heritability of traits, reference population size, average length of chromosomes, relationship between the reference and candidate population, marker density and GEBV estimation method (Song et al., 2023). Thus, it is not easy to draw conclusion about which model is more suitable for the target trait, a better strategy is to evaluate various statistical methods for their performance, select the one with the highest predictive accuracy and use that model for GP.

One of the major roadblocks to the implementation of GS is that the precise prediction of GEBVs require a vast number of markers and the expensive costs associated with genotyping these markers (Goddard and Hayes, 2007; Peñaloza et al., 2022). Thus, selecting the optimal variant panel improves the GP accuracy and reduces genotyping costs. The predictive accuracy showed that the GWAS-*p* strategy was consistently higher than that of Random strategy across all different variance densities. Even at low variance densities, such as 500 SNPs, the prediction accuracy of the GWAS-*p* strategy also exhibited superior accuracy. Specifically, the rrBLUP and SVM models had a maximum prediction accuracy of 0.7734 ± 0.026 at 10 k SNP density and 0.7454 ± 0.0316 at 1 k InDel density, respectively. This might be attributed to the fact that these heat tolerance related SNPs or InDels were detected by GWAS analysis, which explained the majority of the genetic variance. Similar findings have been documented for heat tolerance in abalone (Liu et al., 2022) and Zhikong scallop (Yu et al., 2023), disease resistance in gilthead sea bream (*Sparus aurata*) (Luo et al., 2021), and ammonia tolerance in orange-spotted grouper (*E. coioides*) (Shan et al., 2021). Overall, GWAS-*p* strategy is a feasible and cost-effective method to achieve high prediction accuracy, and we would prefer the rrBLUP and SVM as the optimal models for SNP and InDel markers of thermal tolerance traits in spotted sea bass, respectively.

5. Conclusion

In the present study, genome-wide association study (GWAS) and genomic prediction (GP) were combined to elucidate genetic mechanism underlying thermal tolerance and to estimate the predictive accuracy of ten breeding models in spotted sea bass. As a result, 50 significant variants, including 31 SNPs and 19 InDels, were associated with heat tolerance trait, and annotated 236 candidate genes, among which *hspa5*, *mrpl13* and *ndufs8* were regarded as hub genes. Enrichment results showed that membrane trafficking pathway serves a key role in responding to thermal stress. Furthermore, we compared the predictive accuracies of ten GS models with different marker densities and two marker selection strategies, showing that the GWAS-*p* selection strategy exhibited higher prediction accuracy compared to the Random selection strategy. The rrBLUP and SVM models were identified as the optimal models for GS programs targeting heat tolerance trait in spotted sea bass for SNP and InDel markers, respectively. These findings lay solid foundations for investigation of heat tolerance of spotted sea bass and facilitate the application of GS for heat tolerance trait in aquatic species.

Supplementary data to this article can be found online at https://doi.org/10.1016/j.aquaculture.2024.741951.

Funding

This work was supported by National Key Research and Development Program of China [grant number: 2022YFD2400503] and China Agricufture Research System (CARS for Marine Fish Culture Industry) [grant number: CARS-47-G06].

CRediT authorship contribution statement

Cong Liu: Writing – original draft, Software, Methodology, Conceptualization. **Haishen Wen:** Resources, Funding acquisition, Conceptualization. **Chong Zhang:** Visualization, Methodology. **Yonghang Zhang:** Software, Methodology. **Lingyu Wang:** Software, Methodology. **Donglei Sun:** Software, Data curation. **Mengqun Liu:** Software, Methodology. **Yani Dong:** Visualization, Software. **Pengyu Li:** Visualization, Methodology. **Hao Li:** Software, Methodology. **Kaiqiang Zhang:** Software, Conceptualization. **Xin Qi:** Resources, Methodology. **Yun Li:** Writing – review & editing, Methodology, Funding acquisition.

Declaration of competing interest

The corresponding authors state that there are no conflicts of interest.

Data availability

Data will be made available on request.

References

Alexander, D.H., Novembre, J., Lange, K., 2009. Fast model-based estimation of ancestry in unrelated individuals. Genome Res. 19, 1655–1664. https://doi.org/10.1101/gr.094052.109.

Alfonso, S., Gesto, M., Sadoul, B., 2021. Temperature increase and its effects on fish stress physiology in the context of global warming. J. Fish Biol. 98, 1496–1508. https://doi.org/10.1111/jfb.14599.

Benfey, T., Gonen, S., Bartlett, C., Garber, A., 2022. High heritability for thermal tolerance in atlantic salmon, *Salmo salar*. Res. Sq. https://doi.org/10.21203/rs.3.rs-2347113/v1.

Bennett, G.L., Pollak, E.J., Kuehn, L.A., Snelling, W.M., 2014. Breeding: Animals. In: Van Alfen, N.K. (Ed.), Encyclopedia of Agriculture and Food Systems. Academic Press, Oxford, pp. 173–186.

Breiman, L., 2001. Random forests. Mach. Learn. 45, 5–32. https://doi.org/10.1023/A:1010933404324.

Bu, D., Luo, H., Huo, P., Wang, Z., Zhang, S., He, Z., Wu, Y., Zhao, L., Liu, J., Guo, J., Fang, S., Cao, W., Yi, L., Zhao, Y., Kong, L., 2021. KOBAS-i: intelligent prioritization and exploratory visualization of biological functions for gene enrichment analysis. Nucleic Acids Res. 49, W317–w325. https://doi.org/10.1093/nar/gkab447.

Buckley, B.A., Gracey, A.Y., Somero, G.N., 2006. The cellular response to heat stress in the goby *Gillichthys mirabilis*: a cDNA microarray and protein-level analysis. J. Exp. Biol. 209, 2660–2677. https://doi.org/10.1242/jeb.02292.

Camara, M.D., Yen, S., Kaspar, H.F., Kesarcodi-Watson, A., King, N., Jeffs, A.G., Tremblay, L.A., 2017. Assessment of heat shock and laboratory virus challenges to selectively breed for ostreid herpesvirus 1 (OsHV-1) resistance in the Pacific oyster, *Crassostrea gigas*. Aquaculture 469, 50–58. https://doi.org/10.1016/j.aquaculture.2016.11.031.

Chan, S.K.N., Suresh, S., Munday, P., Ravasi, T., Bernal, M.A., Schunter, C., 2022. The alternative splicing landscape of a coral reef fish during a marine heatwave. Ecol. Evol. 12, e8738. https://doi.org/10.1002/ece3.8738.

Chen, N., Luo, X., Gu, Y., Han, G., Dong, Y., You, W., Ke, C., 2016. Assessment of the thermal tolerance of abalone based on cardiac performance in *Haliotis discus hannai*, *H. gigantea* and their interspecific hybrid. Aquaculture 465, 258–264. https://doi.org/10.1016/j.aquaculture.2016.09.004.

Chen, S., Zhou, Y., Chen, Y., Gu, J., 2018. fastp: an ultra-fast all-in-one FASTQ preprocessor. Bioinformatics 34, i884–i890. https://doi.org/10.1093/bioinformatics/bty560.

Cingolani, P., Platts, A., Wang le, L., Coon, M., Nguyen, T., Wang, L., Land, S.J., Lu, X., Ruden, D.M., 2012. A program for annotating and predicting the effects of single nucleotide polymorphisms, SnpEff: SNPs in the genome of Drosophila melanogaster strain w1118; iso-2; iso-3. Fly, 6, pp. 80–92. https://doi.org/10.4161/fly.19695.

Corey, E., Linnansaari, T., Dugdale, S.J., Bergeron, N., Gendron, J.-F., Lapointe, M., Cunjak, R.A., 2020. Comparing the behavioural thermoregulation response to heat stress by Atlantic salmon parr (*Salmo salar*) in two rivers. Ecol. Freshw. Fish 29, 50–62. https://doi.org/10.1111/eff.12487.

D'Agaro, E., Favaro, A., Matiussi, S., Gibertoni, P.P., Esposito, S., 2021. Genomic selection in salmonids: new discoveries and future perspectives. Aquac. Int. 29, 2259–2289. https://doi.org/10.1007/s10499-021-00747-w.

D'Ambrosio, J., Morvezen, R., Brard-Fudulea, S., Bestin, A., Acin Perez, A., Guéméné, D., Poncet, C., Haffray, P., Dupont-Nivet, M., Phocas, F., 2020. Genetic architecture and genomic selection of female reproduction traits in rainbow trout. BMC Genomics 21, 558. https://doi.org/10.1186/s12864-020-06955-7.

Dittmar, J., Janssen, H., Kuske, A., Kurtz, J., Scharsack, J.P., 2014. Heat and immunity: an experimental heat wave alters immune functions in three-spined sticklebacks (*Gasterosteus aculeatus*). J. Anim. Ecol. 83, 744–757. https://doi.org/10.1111/1365-2656.12175.

Endelman, J.B., 2011. Ridge regression and other kernels for genomic selection with R package rrBLUP. Plant Genome 4. https://doi.org/10.3835/plantgenome2011.08.0024.
Forgati, M., Kandalski, P.K., Herrerias, T., Zaleski, T., Machado, C., Souza, M., Donatti, L., 2017. Effects of heat stress on the renal and branchial carbohydrate metabolism and antioxidant system of Antarctic fish. J. Comp. Physiol. B. 187, 1137–1154. https://doi.org/10.1007/s00360-017-1088-3.
Fraslin, C., Koskinen, H., Nousianen, A., Houston, R.D., Kause, A., 2022. Genome-wide association and genomic prediction of resistance to Flavobacterium columnare in a farmed rainbow trout population. Aquaculture 557, 738332. https://doi.org/10.1016/j.aquaculture.2022.738332.
Gabián, M., Morán, P., Fernández, A.I., Villanueva, B., Chtioui, A., Kent, M.P., Covelo-Soto, L., Fernández, A., Saura, M., 2019. Identification of genomic regions regulating sex determination in Atlantic salmon using high density SNP data. BMC Genomics 20, 764. https://doi.org/10.1186/s12864-019-6104-4.
Gallardo-Hidalgo, J., Barría, A., Yoshida, G.M., Yáñez, J.M., 2021. Genetics of growth and survival under chronic heat stress and trade-offs with growth- and robustness-related traits in rainbow trout. Aquaculture 531, 735685. https://doi.org/10.1016/j.aquaculture.2020.735685.
García-Souto, D., Martínez-Mariño, V., Morán, P., Olabarria, C., Vázquez, E., 2024. Hiding from heat: the transcriptomic response of two clam species is modulated by behaviour and habitat. J. Therm. Biol. 119, 103776. https://doi.org/10.1016/j.jtherbio.2023.103776.
Goddard, M.E., Hayes, B.J., 2007. Genomic selection. J. Anim. Breed. Genet. 124, 323–330. https://doi.org/10.1111/j.1439-0388.2007.00702.x.
Gong, J., Zhao, J., Ke, Q., Li, B., Zhou, Z., Wang, J., Zhou, T., Zheng, W., Xu, P., 2022. First genomic prediction and genome-wide association for complex growth-related traits in rock bream (*Oplegnathus fasciatus*). Evol. Appl. 15, 523–536. https://doi.org/10.1111/eva.13218.
Haack, T.B., Haberberger, B., Frisch, E.-M., Wieland, T., Iuso, A., Gorza, M., Strecker, V., Graf, E., Mayr, J.A., Herberg, U., Hennermann, J.B., Klopstock, T., Kuhn, K.A., Ahting, U., Sperl, W., Wilichowski, E., Hoffmann, G.F., Tesarova, M., Hansikova, H., Zeman, J., Plecko, B., Zeviani, M., Wittig, I., Strom, T.M., Schuelke, M., Freisinger, P., Meitinger, T., Prokisch, H., 2012. Molecular diagnosis in mitochondrial complex I deficiency using exome sequencing. J. Med. Genet. 49, 277. https://doi.org/10.1136/jmedgenet-2012-100846.
Hao, Y., Cui, Y., Gu, X., 2016. Genome-wide DNA methylation profiles changes associated with constant heat stress in pigs as measured by bisulfite sequencing. Sci. Rep. 6, 27507. https://doi.org/10.1038/srep27507.
Hazel, J.R., 1995. Thermal adaptation in biological membranes: is Homeoviscous adaptation the explanation? Annu. Rev. Physiol. 57, 19–42. https://doi.org/10.1146/annurev.ph.57.030195.000315.
Holborn, M.K., Ang, K.P., Elliott, J.A.K., Powell, F., Boulding, E.G., 2018. Genome wide association analysis for bacterial kidney disease resistance in a commercial north American Atlantic salmon (*Salmo salar*) population using a 50 K SNP panel. Aquaculture 495, 465–471. https://doi.org/10.1016/j.aquaculture.2018.06.014.
Iftikar, F.I., Morash, A.J., Cook, D.G., Herbert, N.A., Hickey, A.J.R., 2015. Temperature acclimation of mitochondria function from the hearts of a temperate wrasse (*Notolabrus celidotus*). Comp. Biochem. Physiol. A Mol. Integr. Physiol. 184, 46–55. https://doi.org/10.1016/j.cbpa.2015.01.017.
Islam, M.J., Kunzmann, A., Slater, M.J., 2022. Responses of aquaculture fish to climate change-induced extreme temperatures: a review. J. World Aquacult. Soc. 53, 314–366. https://doi.org/10.1111/jwas.12853.
Jerome, H.F., 2001. Greedy function approximation: a gradient boosting machine. Ann. Stat. 29, 1189–1232. https://doi.org/10.1214/aos/1013203451.
Jeyachandran, S., Chellapandian, H., Park, K., Kwak, I.-S., 2023. A review on the involvement of heat shock proteins (extrinsic chaperones) in response to stress conditions in aquatic organisms. Antioxidants 12 (7). https://doi.org/10.3390/antiox12071444.
Jia, Y., Chen, X., Wang, Z., Meng, Z., Huang, B., Guan, C., 2020. Physiological response of juvenile turbot (*Scophthalmus maximus.* L) during hyperthermal stress. Aquaculture 529, 735645. https://doi.org/10.1016/j.aquaculture.2020.735645.
Jiang, Y., Guo, J., Haisa, A., Shen, Y., 2022. Genome-wide association analysis of heat tolerance in the northern pike (*Esox Lucius*). Aquaculture 559, 738459. https://doi.org/10.1016/j.aquaculture.2022.738459.
Jin, Y., Zhou, T., Geng, X., Liu, S., Chen, A., Yao, J., Jiang, C., Tan, S., Su, B., Liu, Z., 2017. A genome-wide association study of heat stress-associated SNPs in catfish. Anim. Genet. 48, 233–236. https://doi.org/10.1111/age.12482.
Jing, C., Fu, R., Wang, C., Li, X., Zhang, W., 2021. MRPL13 act as a novel therapeutic target and could promote cell proliferation in non-small cell lung Cancer. Cancer Manag. Res. 13, 5535–5545. https://doi.org/10.2147/CMAR.S316428.
Karatzoglou, A., Smola, A., Hornik, K., Zeileis, A., 2004. kernlab - An S4 Package for Kernel Methods in R. J. Stat. Softw. 11, 1–20. https://doi.org/10.18637/jss.v011.i09.
Ke, Q., Wang, J., Bai, Y., Zhao, J., Gong, J., Deng, Y., Qu, A., Suo, N., Chen, J., Zhou, T., Xu, P., 2022. GWAS and genomic prediction revealed potential for genetic improvement of large yellow croaker adapting to high plant protein diet. Aquaculture 553, 738090. https://doi.org/10.1016/j.aquaculture.2022.738090.
Kim, D., Langmead, B., Salzberg, S.L., 2015. HISAT: a fast spliced aligner with low memory requirements. Nat. Methods 12, 357–360. https://doi.org/10.1038/nmeth.3317.
Kim, W.-J., Lee, K., Lee, D., Kim, H.-C., Nam, B.-H., Jung, H., Yi, S.-J., Kim, K., 2021. Transcriptome profiling of olive flounder responses under acute and chronic heat stress. GENES GENOM 43, 151–159. https://doi.org/10.1007/s13258-021-01053-8.
Kobayashi, M., Msangi, S., Batka, M., Vannuccini, S., Dey, M.M., Anderson, J.L., 2015. Fish to 2030: the role and opportunity for aquaculture. Aquac. Econ. Manag. 19, 282–300. https://doi.org/10.1080/13657305.2015.994240.
Kong, S., Zhou, Z., Zhou, T., Zhao, J., Chen, L., Lin, H., Pu, F., Ke, Q., Bai, H., Xu, P., 2020. Genome-wide association study of body shape-related traits in large yellow croaker (*Larimichthys crocea*). Mar. Biotechnol. 22, 631–643. https://doi.org/10.1007/s10126-020-09983-2.
Korte, A., Farlow, A., 2013. The advantages and limitations of trait analysis with GWAS: a review. Plant Methods 9, 29. https://doi.org/10.1186/1746-4811-9-29.
Kumar, V., Roy, S., Behera, B.K., Das, B.K., 2022. Heat shock proteins (Hsps) in cellular homeostasis: a promising tool for health Management in Crustacean Aquaculture. Life 12 (11). https://doi.org/10.3390/life12111777.
Lagarde, H., Lallias, D., Patrice, P., Dehaullon, A., Prchal, M., François, Y., D'Ambrosio, J., Segret, E., Acin-Perez, A., Cachelou, F., Haffray, P., Dupont-Nivet, M., Phocas, F., 2023. Genetic architecture of acute hyperthermia resistance in juvenile rainbow trout (*Oncorhynchus mykiss*) and genetic correlations with production traits. Genet. Sel. Evol. 55, 39. https://doi.org/10.1186/s12711-023-00811-4.
Li, H., 2013. Aligning sequence reads, clone sequences and assembly contigs with BWA-MEM. arXiv Genomics. https://doi.org/10.48550/arXiv.1303.3997.
Lippincott-Schwartz, J., Roberts, T.H., Hirschberg, K., 2000. Secretory protein trafficking and organelle dynamics in living cells. Annu. Rev. Cell Dev. Biol. 16, 557–589. https://doi.org/10.1146/annurev.cellbio.16.1.557.
Liu, Y., Lu, S., Liu, F., Shao, C., Zhou, Q., Wang, N., Li, Y., Yang, Y., Zhang, Y., Sun, H., Zheng, W., Chen, S., 2018. Genomic selection using BayesCπ and GBLUP for resistance against Edwardsiella tarda in Japanese flounder (*Paralichthys olivaceus*). Mar. Biotechnol. 20, 559–565. https://doi.org/10.1007/s10126-018-9839-z.
Liu, G., Dong, L., Gu, L., Han, Z., Zhang, W., Fang, M., Wang, Z., 2019. Evaluation of genomic selection for seven economic traits in yellow drum (*Nibea albiflora*). Mar. Biotechnol. 21, 806–812. https://doi.org/10.1007/s10126-019-09925-7.
Liu, J., Peng, W., Yu, F., Shen, Y., Yu, W., Lu, Y., Lin, W., Zhou, M., Huang, Z., Luo, X., You, W., Ke, C., 2022. Genomic selection applications can improve the environmental performance of aquatics: a case study on the heat tolerance of abalone. Evol. Appl. 15, 992–1001. https://doi.org/10.1111/eva.13388.
Logan, C.A., Somero, G.N., 2011. Effects of thermal acclimation on transcriptional responses to acute heat stress in the eurythermal fish *Gillichthys mirabilis* (Cooper). Am. J. Phys. Regul. Integr. Comp. Phys. 300, R1373–R1383. https://doi.org/10.1152/ajpregu.00689.2010.
Love, M.I., Huber, W., Anders, S., 2014. Moderated estimation of fold change and dispersion for RNA-seq data with DESeq2. Genome Biol. 15, 550. https://doi.org/10.1186/s13059-014-0550-8.
Luo, Z., Yu, Y., Xiang, J., Li, F., 2021. Genomic selection using a subset of SNPs identified by genome-wide association analysis for disease resistance traits in aquaculture species. Aquaculture 539, 736620. https://doi.org/10.1016/j.aquaculture.2021.736620.
Lyu, L., Wen, H., Li, Y., Li, J., Zhao, J., Zhang, S., Song, M., Wang, X., 2018. Deep transcriptomic analysis of black rockfish (*Sebastes schlegelii*) provides new insights on responses to acute temperature stress. Sci. Rep. 8, 9113. https://doi.org/10.1038/s41598-018-27013-z.
Ma, A., Wang, X.A., Huang, Z., Liu, Z., Cui, W., Qu, J., 2018. Estimation of genetic parameters for upper thermal tolerance and growth-related traits in turbot *Scophthalmus maximus* using the Bayesian method based on Gibbs sampling. Acta Pharmacol. Sin. 37, 40–46. https://doi.org/10.1007/s13131-018-1185-5.
Marquez-Acevedo, A.S., Hood, W.R., Collier, R.J., Skibiel, A.L., 2023. Graduate student literature review: mitochondrial response to heat stress and its implications on dairy cattle bioenergetics, metabolism, and production. J. Dairy Sci. 106, 7295–7309. https://doi.org/10.3168/jds.2023-23340.
McKenna, A., Hanna, M., Banks, E., Sivachenko, A., Cibulskis, K., Kernytsky, A., Garimella, K., Altshuler, D., Gabriel, S., Daly, M., DePristo, M.A., 2010. The genome analysis toolkit: a MapReduce framework for analyzing next-generation DNA sequencing data. Genome Res. 20, 1297–1303. https://doi.org/10.1101/gr.107524.110.
Meuwissen, T., Hayes, B., Goddard, M., 2013. Accelerating improvement of livestock with genomic selection. Annu. Rev. Anim. Biosci. 1, 221–237. https://doi.org/10.1146/annurev-animal-031412-103705.
Naylor, R.L., Kishore, A., Sumaila, U.R., Issifu, I., Hunter, B.P., Belton, B., Bush, S.R., Cao, L., Gelcich, S., Gephart, J.A., Golden, C.D., Jonell, M., Koehn, J.Z., Little, D.C., Thilsted, S.H., Tigchelaar, M., Crona, B., 2021. Blue food demand across geographic and temporal scales. Nat. Commun. 12, 5413. https://doi.org/10.1038/s41467-021-25516-4.
Ødegård, J., Baranski, M., Gjerde, B., Gjedrem, T., 2011. Methodology for genetic evaluation of disease resistance in aquaculture species: challenges and future prospects. Aquac. Res. 42, 103–114. https://doi.org/10.1111/j.1365-2109.2010.02669.x.
Omeka, W.K.M., Liyanage, D.S., Lee, S., Lim, C., Yang, H., Sandamalika, W.M.G., Udayantha, H.M.V., Kim, G., Ganeshalingam, S., Jeong, T., Oh, S.-R., Won, S.-H., Koh, H.-B., Kim, M.-K., Jones, D.B., Massault, C., Jerry, D.R., Lee, J., 2022. Genome-wide association study (GWAS) of growth traits in olive flounder (*Paralichthys olivaceus*). Aquaculture 555, 738257. https://doi.org/10.1016/j.aquaculture.2022.738257.
Paul, K., Restoux, G., Phocas, F., 2022. Genome-wide detection of positive and balancing selection signatures shared by four domesticated rainbow trout populations (*Oncorhynchus mykiss*). bioRxiv 2022. https://doi.org/10.1101/2022.12.08.519621, 2012.2008.519621.
Peñaloza, C., Barria, A., Papadopoulou, A., Hooper, C., Preston, J., Green, M., Helmer, L., Kean-Hammerson, J., Nascimento-Schulze, J.C., Minardi, D., Gundappa, M.K.,

Macqueen, D.J., Hamilton, J., Houston, R.D., Bean, T.P., 2022. Genome-wide association and genomic prediction of growth traits in the European flat oyster (*Ostrea edulis*). Front. Genet. 13. https://doi.org/10.3389/fgene.2022.926638.

Pérez-Rodríguez, P., de los Campos, G., 2022. Multitrait Bayesian shrinkage and variable selection models with the BGLR-R package. Genetics 222, iyac112. https://doi.org/10.1093/genetics/iyac112.

Purcell, S., Neale, B., Todd-Brown, K., Thomas, L., Ferreira, M.A., Bender, D., Maller, J., Sklar, P., de Bakker, P.I., Daly, M.J., Sham, P.C., 2007. PLINK: a tool set for whole-genome association and population-based linkage analyses. Am. J. Hum. Genet. 81, 559–575. https://doi.org/10.1086/519795.

Qian, B., Xue, L., 2016. Liver transcriptome sequencing and de novo annotation of the large yellow croaker (*Larimichthy crocea*) under heat and cold stress. Mar. Genomics 25, 95–102. https://doi.org/10.1016/j.margen.2015.12.001.

Rebl, A., Verleih, M., Köbis, J.M., Kühn, C., Wimmers, K., Köllner, B., Goldammer, T., 2013. Transcriptome profiling of gill tissue in regionally bred and globally farmed rainbow trout strains reveals different strategies for coping with thermal stress. Mar. Biotechnol. 15, 445–460. https://doi.org/10.1007/s10126-013-9501-8.

Robledo, D., Matika, O., Hamilton, A., Houston, R.D., 2018. Genome-wide association and genomic selection for resistance to amoebic gill disease in Atlantic Salmon. G3: Genes Genomes Genet. 8, 1195–1203. https://doi.org/10.1534/g3.118.200075.

San, L.-Z., Liu, B.-S., Liu, B., Zhu, K.-C., Guo, L., Guo, H.-Y., Zhang, N., Jiang, S.-G., Zhang, D.-C., 2021. Genome-wide association study reveals multiple novel SNPs and putative candidate genes associated with low oxygen tolerance in golden pompano *Trachinotus ovatus* (Linnaeus 1758). Aquaculture 544, 737098. https://doi.org/10.1016/j.aquaculture.2021.737098.

Shan, X., Xu, T., Ma, Z., Zhang, X., Ruan, Z., Chen, J., Shi, Q., You, X., 2021. Genome-wide association improves genomic selection for ammonia tolerance in the orange-spotted grouper (*Epinephelus coioides*). Aquaculture 533, 736214. https://doi.org/10.1016/j.aquaculture.2020.736214.

Shim, H., Chasman, D.I., Smith, J.D., Mora, S., Ridker, P.M., Nickerson, D.A., Krauss, R. M., Stephens, M., 2015. A multivariate genome-wide association analysis of 10 LDL subfractions, and their response to statin treatment, in 1868 Caucasians. PLoS One 10, e0120758. https://doi.org/10.1371/journal.pone.0120758.

Shumate, A., Wong, B., Pertea, G., Pertea, M., 2022. Improved transcriptome assembly using a hybrid of long and short reads with StringTie. PLoS Comput. Biol. 18, e1009730. https://doi.org/10.1371/journal.pcbi.1009730.

Song, J., McDowell, J.R., 2021. Comparative transcriptomics of spotted seatrout (*Cynoscion nebulosus*) populations to cold and heat stress. Ecol. Evol. 11, 1352–1367. https://doi.org/10.1002/ece3.7138.

Song, H., Dong, T., Yan, X., Wang, W., Tian, Z., Sun, A., Dong, Y., Zhu, H., Hu, H., 2023. Genomic selection and its research progress in aquaculture breeding. Rev. Aquac. 15, 274–291. https://doi.org/10.1111/raq.12716.

Stenmark, H., 2009. Rab GTPases as coordinators of vesicle traffic. Nat. Rev. Mol. Cell Biol. 10, 513–525. https://doi.org/10.1038/nrm2728.

Sukhavachana, S., Tongyoo, P., Massault, C., McMillan, N., Leungnaruemitchai, A., Poompuang, S., 2020. Genome-wide association study and genomic prediction for resistance against Streptococcus agalactiae in hybrid red tilapia (*Oreochromis spp.*). Aquaculture 525, 735297. https://doi.org/10.1016/j.aquaculture.2020.735297.

Sun, Y., Wen, H., Tian, Y., Mao, X., Li, X., Li, J., Hu, Y., Liu, Y., Li, J., Li, Y., 2021. HSP90 and HSP70 families in Lateolabrax maculatus: genome-wide identification, molecular characterization, and expression profiles in response to various environmental stressors. Front. Physiol. 12. https://doi.org/10.3389/fphys.2021.784803.

Tang, H., Liu, J., Wang, Z., Zhang, L., Yang, M., Huang, J., Wen, X., Luo, J., 2023. Genome-wide association study (GWAS) analysis of black color trait in the leopard coral grouper (*Plectropomus leopardus*) using whole genome resequencing. Comp. Biochem. Physiol. Part D Genomics Proteomics 48, 101138. https://doi.org/10.1016/j.cbd.2023.101138.

Udayantha, H.M.V., Lee, S., Liyanage, D.S., Lim, C., Jeong, T., Omeka, W.K.M., Yang, H., Kim, G., Kim, J., Lee, J., Nadarajapillai, K., Ganeshalingam, S., Park, C.-U., Lee, J., Oh, S.-R., Gong, P., Jang, Y., Hyun, J., Park, A., Koh, H.-B., Kim, M.-K., Jones, D.B., Massault, C., Jerry, D.R., Lee, J., 2023. Identification of candidate variants and genes associated with temperature tolerance in olive flounders by genome-wide association study (GWAS). Aquaculture 576, 739858. https://doi.org/10.1016/j.aquaculture.2023.739858.

VanRaden, P.M., 2008. Efficient methods to compute genomic predictions. J. Dairy Sci. 91, 4414–4423. https://doi.org/10.3168/jds.2007-0980.

Vela-Avitúa, S., Thorland, I., Bakopoulos, V., Papanna, K., Dimitroglou, A., Kottaras, E., Leonidas, P., Guinand, B., Tsigenopoulos, C.S., Aslam, M.L., 2022. Genetic basis for resistance against viral nervous necrosis: GWAS and potential of genomic prediction explored in farmed European Sea bass (*Dicentrarchus labrax*). Front. Genet. 13. https://doi.org/10.3389/fgene.2022.804584.

Vermeer, M., Rahmstorf, S., 2009. Global sea level linked to global temperature. Proc. Natl. Acad. Sci. USA 106, 21527–21532. https://doi.org/10.1073/pnas.0907765106.

Wang, Y., Li, C., Pan, C., Liu, E., Zhao, X., Ling, Q., 2019. Alterations to transcriptomic profile, histopathology, and oxidative stress in liver of pikeperch (*Sander lucioperca*) under heat stress. Fish Shellfish Immunol. 95, 659–669. https://doi.org/10.1016/j.fsi.2019.11.014.

Wang, Y., Su, C., Liu, Q., Hao, X., Han, S., Doretto, L.B., Rosa, I.F., Yang, Y., Shao, C., Wang, Q., 2024. Transcriptome analysis revealed the early heat stress response in the brain of Chinese tongue sole (*Cynoglossus semilaevis*). Animals 14. https://doi.org/10.3390/ani14010084.

Wu, Y., Zhou, Z., Pan, Y., Zhao, J., Bai, H., Chen, B., Zhang, X., Pu, F., Chen, J., Xu, P., 2021. GWAS identified candidate variants and genes associated with acute heat tolerance of large yellow croaker. Aquaculture 540, 736696. https://doi.org/10.1016/j.aquaculture.2021.736696.

Xu, Y., Ma, K., Zhao, Y., Wang, X., Zhou, K., Yu, G., Li, C., Li, P., Yang, Z., Xu, C., Xu, S., 2021. Genomic selection: a breakthrough technology in rice breeding. Crop J. 9, 669–677. https://doi.org/10.1016/j.cj.2021.03.008.

Yang, J., Lee, S.H., Goddard, M.E., Visscher, P.M., 2011. GCTA: a tool for genome-wide complex trait analysis. Am. J. Hum. Genet. 88, 76–82. https://doi.org/10.1016/j.ajhg.2010.11.011.

Yang, Y., Wu, L., Wu, X., Li, B., Huang, W., Weng, Z., Lin, Z., Song, L., Guo, Y., Meng, Z., Liu, X., Xia, J., 2020a. Identification of candidate growth-related SNPs and genes using GWAS in Brown-marbled grouper (*Epinephelus fuscoguttatus*). Mar. Biotechnol. 22, 153–166. https://doi.org/10.1007/s10126-019-09940-8.

Yang, S., Zhao, T., Ma, A., Huang, Z., Liu, Z., Cui, W., Zhang, J., Zhu, C., Guo, X., Yuan, C., 2020b. Metabolic responses in *Scophthalmus maximus* kidney subjected to thermal stress. Fish Shellfish Immunol. 103, 37–46. https://doi.org/10.1016/j.fsi.2020.04.003.

Yin, L., Zhang, H., Tang, Z., Xu, J., Yin, D., Zhang, Z., Yuan, X., Zhu, M., Zhao, S., Li, X., Liu, X., 2021. rMVP: a memory-efficient, visualization-enhanced, and parallel-accelerated tool for genome-wide association study. Genomics Proteomics Bioinformatics 19, 619–628. https://doi.org/10.1016/j.gpb.2020.10.007.

Yoshida, G.M., Yáñez, J.M., 2022. Increased accuracy of genomic predictions for growth under chronic thermal stress in rainbow trout by prioritizing variants from GWAS using imputed sequence data. Evol. Appl. 15, 537–552. https://doi.org/10.1111/eva.13240.

Yoshida, G.M., Lhorente, J.P., Correa, K., Soto, J., Salas, D., Yáñez, J.M., 2019. Genome-wide association study and cost-efficient genomic predictions for growth and fillet yield in Nile Tilapia (*Oreochromis niloticus*). G3: Genes Genomes Genet. 9, 2597–2607. https://doi.org/10.1534/g3.119.400116.

Yu, F., Peng, W., Tang, B., Zhang, Y., Wang, Y., Gan, Y., Luo, X., You, W., Gwo, J.-C., Chen, N., Ke, C., 2021. A genome-wide association study of heat tolerance in Pacific abalone based on genome resequencing. Aquaculture 536, 736436. https://doi.org/10.1016/j.aquaculture.2021.736436.

Yu, H., Sui, M., Yang, Z., Cui, C., Hou, X., Liu, Z., Wang, X., Dong, X., Zhao, A., Wang, Y., Huang, X., Hu, J., Bao, Z., 2023. Deciphering the genetic basis and prediction genomic estimated breeding values of heat tolerance in Zhikong scallop *Chlamys farreri*. Aquaculture 565, 739090. https://doi.org/10.1016/j.aquaculture.2022.739090.

Yu, Y., Wan, S.-M., Zhang, S.-M., Liu, J.-Q., Sun, A.-L., Wang, Y., Zhu, Y.-F., Gu, S.-X., Gao, Z.-X., 2024. Identification of SNPs and candidate genes associated with growth using GWAS and transcriptome analysis in *Coilia nasus*. Aquaculture 586, 740777. https://doi.org/10.1016/j.aquaculture.2024.740777.

Zhang, C., Dong, S.-S., Xu, J.-Y., He, W.-M., Yang, T.-L., 2019. PopLDdecay: a fast and effective tool for linkage disequilibrium decay analysis based on variant call format files. Bioinformatics 35, 1786–1788. https://doi.org/10.1093/bioinformatics/bty875.

Zhang, W., Xu, X., Li, J., Shen, Y., 2022. Transcriptomic analysis of the liver and brain in grass carp (*Ctenopharyngodon idella*) under heat stress. Mar. Biotechnol. 24, 856–870. https://doi.org/10.1007/s10126-022-10148-6.

Zhang, C., Wen, H., Zhang, Y., Zhang, K., Qi, X., Li, Y., 2023. First genome-wide association study and genomic prediction for growth traits in spotted sea bass (*Lateolabrax maculatus*) using whole-genome resequencing. Aquaculture 566, 739194. https://doi.org/10.1016/j.aquaculture.2022.739194.

Zhao, X., Li, L., Li, C., Liu, E., Zhu, H., Ling, Q., 2022. Heat stress-induced endoplasmic reticulum stress promotes liver apoptosis in largemouth bass (*Micropterus salmoides*). Aquaculture 546, 737401. https://doi.org/10.1016/j.aquaculture.2021.737401.

Zhou, X., Stephens, M., 2012. Genome-wide efficient mixed-model analysis for association studies. Nat. Genet. 44, 821–824. https://doi.org/10.1038/ng.2310.

Zhou, Y., Fu, B., Yu, X., Chen, G., Wang, J., Luo, W., Feng, Y., Tong, J., 2021a. Genome-wide association study reveals genomic regions and candidate genes for head size and shape in bighead carp (*Hypophthalmichthys nobilis*). Aquaculture 539, 736648. https://doi.org/10.1016/j.aquaculture.2021.736648.

Zhou, C.-Q., Ka, W., Yuan, W.-K., Wang, J.-L., 2021b. The effect of acute heat stress on the innate immune function of rainbow trout based on the transcriptome. J. Therm. Biol. 96, 102834. https://doi.org/10.1016/j.jtherbio.2021.102834.

Zhu, X., Ni, P., Xing, Q., Wang, Y., Huang, X., Hu, X., Hu, J., Wu, X.-L., Bao, Z., 2021. Genomic prediction of growth traits in scallops using convolutional neural networks. Aquaculture 545, 737171. https://doi.org/10.1016/j.aquaculture.2021.737171.